Editorial Manager(tm) for Bulletin of the Seismological Society of America
Manuscript Draft

Manuscript Number: BSSA-D-09-00046R1

Title: Do strike-slip faults of Molise, central-southern Italy, really release a high stress?

Article Type: Article

Section/Category: Regular Issue

Corresponding Author: Mrs. giovanna calderoni,

Corresponding Author's Institution: Istituto Nazionale di Geofisica e Vulcanologia

First Author: giovanna calderoni

Order of Authors: giovanna calderoni; Antonio Rovelli; Giuliano Milana; Gianluca Valensise

Abstract: The 31 October and 1 November 2002, Molise earthquakes (both Mw 5.7) were caused by right-lateral slip between 12 and 20 km depth. These earthquakes are the result of large-scale reactivation of pre-existing, left-lateral, regionally extended E-W structures of Mesozoic age. Although recorded ground motions were generally smaller than expected for typical Italian earthquakes, a recent paper attributes a stress drop as high as 180 bars to the Molise earthquakes.
We remark that a high stress drop is in contrast both with the relatively long source duration inferred in previous investigations and with geodetic evidence for a significantly smaller fault slip compared with other Apennines earthquakes having similarly large rupture area (e.g. 1997 Umbria-Marche earthquakes).
We analyzed both ground acceleration spectra of the mainshocks and single-station spectral ratios of broad-band seismograms in an extended magnitude range ($2.7 \leq Mw \leq 5.7$). Our results show that neither the spectral amplitudes of recorded ground motions nor the spectral ratios can be fit by a high stress drop source. Instead we find that the observations are consistent with a low stress drop, our best estimates ranging between 6 and 25 bars, in agreement with the relatively long source duration and small coseismic slip.
We interpret the low stress of the 2002 Molise earthquakes in terms of lower energy release mechanisms due to the reutilization of faults reactivated opposite to their original sense of slip.

Suggested Reviewers:

Opposed Reviewers:

Response to Reviewers: A letter will be uploaded.

Copyright Form

This piece of the submission is being sent via mail.

Do strike-slip faults of Molise, central-southern Italy, really release a high stress?

Giovanna Calderoni, Antonio Rovelli, Giuliano Milana, and Gianluca Valensise

Istituto Nazionale di Geofisica e Vulcanologia, Sezione di Sismologia e Tettonofisica, Via di Vigna Murata 605, 00143 Rome, Italy

E-mail: calderoni@ingv.it, rovelli@ingv.it, milana@ingv.it, valensise@ingv.it

Abstract

The 31 October and 1 November 2002, Molise earthquakes (both M_W 5.7) were caused by right-lateral slip between 12 and 20 km depth. These earthquakes are the result of large-scale reactivation of pre-existing, left-lateral, regionally extended E-W structures of Mesozoic age. Although recorded ground motions were generally smaller than expected for typical Italian earthquakes, a recent paper attributes a stress drop as high as 180 bars to the Molise earthquakes. We remark that a high stress drop is in contrast both with the relatively long source duration inferred in previous investigations and with geodetic evidence for a significantly smaller fault slip compared with other Apennines earthquakes having similarly large rupture area (e.g. 1997 Umbria-Marche earthquakes).

We analyzed both ground acceleration spectra of the mainshocks and single-station spectral ratios of broad-band seismograms in an extended magnitude range ($2.7 \leq M_W \leq 5.7$). Our results show that neither the spectral amplitudes of recorded ground motions nor the spectral ratios can be fit by a high stress drop source. Instead we find that the observations are consistent with a low stress drop, our best estimates ranging between 6 and 25 bars, in agreement with the relatively long source duration and small coseismic slip.

We interpret the low stress of the 2002 Molise earthquakes in terms of lower energy release mechanisms due to the reutilization of faults reactivated opposite to their original sense of slip.

Introduction

On 31 October 2002, a M_w 5.7 earthquake occurred in Apulian foreland of Italy (Figure 1), at the border between the Molise and Puglia administrative regions (Maffei and Bazzurro, 2004, and papers therein; Chiarabba *et al.*, 2005). Its macroseismic effects reached MCS intensity VII in the epicentral area and were moderate to low all around it (Galli and Molin, 2004). A distinctive exception was the town of San Giuliano di Puglia, where an instrumentally well documented local site effect (Cara *et al.*, 2005) caused an intensity anomaly. Four distinct microzones of San Giuliano di Puglia suffered damage varying from EMS intensity VI-VII to VIII (Dolce *et al.*, 2004; Goretti, 2006). The zone of strongest damage coincides with the zone where Cara *et al.* (2005) observed the largest amplification using aftershock records. It is an area as small as 0.1 km^2, where 30 people were killed and 173 suffered injuries that required hospitalization. On 1 November a twin earthquake M_w 5.7 occurred about 8 km west of the previous event (Figure 1). This further shock hit mostly uninhabited houses in the epicentral area, yet 56 additional injuries were counted mostly due to panic during the rescue operations from the previous shock. Overall 4,800 residents were evacuated from 8 villages in the epicentral area, including the entire population of San Giuliano di Puglia (nearly 1,200 people).

The two mainshocks were characterized by pure right-lateral strike slip over a previously undetected east-west striking fault at a depth ranging from 12 to 20 km (DISS Working Group, 2007; Chiarabba *et al.*, 2005). They were preceded by two strongly felt foreshocks, and perceptible aftershocks continued for months culminating with a M_D 4.2 event on 1 June 2003. The aftershocks showed a distinct east-west elongation (Chiarabba *et al*., 2005), thus supporting the inferred source mechanism on an independent basis.

Many accelerographs of the Italian accelerometric network were triggered by the strongest shocks of the Molise sequence. In particular, 12 and 9 accelerograms were recorded during the first and second mainshock, respectively (Gorini *et al*., 2004). A comparison of observed ground motions with predictions based on the Sabetta and Pugliese (1987) regression (hereafter SP87) reveals that most of the ground accelerations recorded during the two mainshocks fall significantly below statistical expectations (Figure 2). Three stations located in the distance range 20 to 60 km and having a threshold at 10 gals on the vertical component were not triggered at all (see Figure 2), thus confirming the relatively low level of ground motion. Using the Boore *et al.* (1997) predictive equations, which were specifically derived for strike-slip earthquakes, confirms the anomalously low observed ground accelerations (Figure 2). Not unexpectedly, the intensity-based estimates of the magnitude are 5.2 and 5.3, respectively for the 31 October and 1 November shocks (see Italy's Database of Macroseismic Intensities, v. 2008: http://emidius.mi.ingv.it/DBMI08/). Further

evidence for low strength shaking is supplied by the available estimates of M_L (5.4 and 5.3 for the first and second shock, respectively: http://mednet.rm.ingv.it), both being smaller than the corresponding M_W whereas the expectation is that M_L and M_W are similar for moderate magnitude events (Hanks and Boore, 1984). This is confirmed to occur for normal-faulting earthquakes in the Apennines (Cocco and Rovelli, 1989). Recently two parallel studies (Bindi *et al.*, 2009, and Di Alessandro *et al.*, 2008) assessed the intra-event variability among the strongest earthquakes recorded in Italy. Although the statistical approach of these studies is different, both of them conclude that the 2002 Molise earthquakes present the largest negative residuals.

There are two possible causes for such weak ground motions during the Molise earthquakes: *i)* propagation paths were characterized by stronger attenuation, and/or *ii)* the energy released by the source – and hence the stress drop – was smaller than that observed for the similar-size earthquakes used by SP87 to determine their regression. Inferences from geodetic measurements are in favor of a low stress drop. According to the DISS database (DISS Working Group, 2007), the total fault area that slipped in the 31 October and 1 November mainshocks is about 160 km^2. Based on GPS data, Giuliani *et al.* (2007) inferred an average coseismic slip of 12 cm over a 225 km^2 fault surface. This slip/rupture-area ratio is significantly smaller than that found for other Apennines earthquakes, e.g. the 1997 Umbria-Marche (central Apennines) sequence. The two 26 September mainshocks (M_w 5.7 and 6.0) of that sequence are the largest well-documented earthquakes to have occurred in Italy prior to 2002. They ruptured a total fault surface of 166 km^2 and, according to various workers (e.g. De Martini *et al.*, 2003), geodetically documented average coseismic slip for the 1997 shocks is in the range 30 to 40 cm. The slip/rupture-area ratio of the Colfiorito fault is therefore three times larger than the ratio of the Molise earthquakes. Correspondingly, the static stress drop is about 3 bars for the 2002 Molise and about 10 bars for the 1997 Colfiorito earthquakes. Further evidence for a lower stress drop in the Molise earthquakes is supplied by the comparatively long (5.5 and 3.6 s) source duration estimated by Vallée and Di Luccio (2005) for the 31 October and 1 November events, respectively.

In a recent paper, Malagnini and Mayeda (2008; hereinafter MM08) assessed the source scaling of the 2002 Molise earthquakes based on coda envelopes. In striking contrast with the evidence for low stress drop described above, they found that the mainshocks and some of the aftershocks scale following a high stress drop model (up to 180 bars). MM08 acknowledged the weak shaking caused by these earthquakes, but contended that the cause for the recorded small ground motions is a velocity inversion occurring just above the two mainshock hypocenters and related to the under thrusting of the Apulian platform beneath the Apennines (Chiarabba *et al.*, 2005). In their

interpretation, the velocity inversion reflects downward part of the energy carried out by direct waves, thus explaining the weak shaking observed.

In the framework of a global compilation based on teleseismic waves, Allmann and Shearer (2009) have recently proposed a stress-drop larger than a wordlwide average of 40 bars for the Molise earthquakes. These contrasting conclusions show that the stress drop of the 2002 Molise earthquakes requires further investigations. A correct assessment of the stress drop has important implications for the assessment of ground shaking from future earthquakes and for proper scaling of the source size of large historical earthquakes in one of the most active areas of Italy.

We started off by using seismograms of the main shocks and of the aftershocks written by a seismological station (ARC1) installed in the town of Benevento, 60 km south of the epicenter, to infer source scaling. Its medium-range epicentral distance makes ARC1 especially suitable for a study that requires a point-source approximation assumption. We computed single-station spectral ratios for two additional seismological stations (AQU and CII) also used by MM08. In our approach, the use of raw data in spectral ratios between mainshock and aftershock spectra eliminates the contribution of propagation in the signals, emphasizing scaling properties and supplying first-hand information on whether the observations are more compatible with a high or low stress drop. Any distortions caused by a velocity inversion will affect the mainshocks and aftershocks to a similar extent and will therefore be eliminated by spectral ratios, if the hypocenters and the focal mechanisms are the same. We also analyzed Fourier amplitude spectra both of the ARC1 seismograms and strong-motion accelerograms recorded at rock-site stations during the Molise earthquakes to check if also the absolute ground motion amplitudes are fit by the stress drop scaling inferred from single-station spectral ratios, comparing our estimates with those proposed by MM08. To account for the velocity inversion we modeled propagation based on the crustal model proposed by Chiarabba *et al*. (2005).

Through these analyses, we find that a low stress drop scaling fits much better both spectral ratios and ground motion amplitudes of seismograms and accelerograms, in agreement with the inferred long source duration and with geodetic evidence for a low slip/rupture-area ratio. This result is consistent with findings by Ekström (1994), who attributed a low stress drop to the 5 May 1990, M_w 5.8 Potenza earthquake, another southern Apennines strike-slip earthquake that shares with 2002 a similar rupture depth (15-25 km) and a similar geodynamic framework. We interpret this common feature of the Molise and Potenza earthquakes in terms of different energy release mechanisms between shallow normal-faulting and deeper strike-slip earthquakes in the Apennines.

Data

Our investigation is mostly based on data gathered by ARC1, one of the seismological stations run by Istituto Nazionale di Geofisica e Vulcanologia (INGV) and operating between February 2000 and December 2004 in Benevento, a town located about 60 km south of the epicentral area. These stations, equipped with a 20-bit MarsLite digitizer and a Lennartz 3D-5s velocity-sensor, were installed for an experiment of urban microzoning (Improta *et al*., 2005; Di Giulio *et al*., 2008) and operated in continuous mode with a sampling frequency of 62.5 Hz. The site geology of ARC1 (an outcrop of stiff cemented Pleistocene conglomerates) was selected by Improta *et al.* (2005) as representative of the bedrock beneath the urban area. All of the stations installed in Benevento recorded on scale the aftershock sequence of October-November 2002, but were saturated by the two mainshocks. For this reason, these stations do not appear in Figure 2. However, at the rock site ARC1 only a limited number of peaks were clipped in the body wave trains. We have carefully checked the effect of saturation in terms of distortion of the real amplitude spectra of the two mainshocks recorded at ARC1 (see Appendix A). Our conclusion is that the underestimation of spectral amplitudes due to clipping is small and can be neglected. Therefore, the velocity time series of ARC1 are used in this article for a source scaling study in an extended ($2.7 \leq M_W \leq 5.7$) moment magnitude range.

The strong-motion accelerograms analyzed in this study are those recorded by the accelerometric network owned by Dipartimento della Protezione Civile (Civil Defense Department) of Italy (available at: http://itaca.mi.ingv.it; Working Group ITACA, 2008). The raw data, with a sampling rate of 200 sps, were pre-processed to remove the baseline trend using the pre-event portion, when available, or otherwise the total length of the record (zero-th order correction as shown in Boore *et al.*, 2002). Following Boore and Bommer (2005), a Butterworth fourth-order acausal high-pass filter was then applied to the signals after cosine tapering and zero-padding, both at the beginning and the end of the record. The length of the zero-padding depended on the order of the filter and on the cut-off frequency. The value of the cut-off frequency was 0.10 and 0.35 Hz for the digital and analog accelerograms, respectively. Details on the adopted accelerogram integration procedure can be found in Paolucci *et al*. (2008).

We also analyzed recordings from two broad-band stations of the MedNet network run by INGV (http://mednet.rm.ingv.it/), namely AQU and CII, respectively located about 130 and 40 km from the source (Figure 1). These stations are equipped with a Q4120 digital-to-analog converter and STS-2 broad-band receiver (Mazza *et al.*, 2008). Their sampling rate is 20 sps.

A summary of the events considered in this work is given in Table 1 along with the relevant stations. Figure 3 shows representative ground motions caused by the 31 October 2002 earthquake.

Methods of analysis

Our analysis consists of two parts. First, we compute single-station spectral ratios using available velocity-sensor records to infer source scaling, checking the consistency of the inferred scaling with absolute amplitude spectra too. Then we estimate source-radiated acceleration spectra using strong-motion accelerograms of mainshocks, thus repeating the source scaling estimate through independent data and equations including the propagation model.

Broad-band seismograms of ARC1, AQU, and CII were used for the computation of spectral ratios. The frequency band of analysis was fixed to 0.2-10 Hz depending on the signal-to-noise ratio at small magnitude. The basic assumption of this study is that the recorded ground velocity is the convolution of source, propagation path, and site terms

$$V(f) = \frac{A_0(f)}{2\pi f} \cdot P(f,R) \cdot H(f) \qquad (1)$$

where *V(f)* is the Fourier amplitude spectrum of seismograms after deconvolution of the instrument response. Velocity spectra were assessed by means of the fast Fourier transform of the two horizontal components. We used a time window beginning 1 to 2 seconds before the shear wave arrival and including the most significant part of the seismograms with a duration of 10 to 30 s (time window increases with event magnitude). Different criteria are used in the literature for time windowing: we adopted decreasing durations for decreasing magnitude to prevent overestimation of the denominator spectrum which could lead to underestimation of the mainshock stress drop. A 10% cosine taper was applied. The square of the two horizontal motion spectra were summed and the square-root was computed. The final result was smoothed with a running mean over 0.1 Hz.

In (1), $A_0(f)$ and *H(f)* are the source radiated acceleration and the site transfer function, respectively, whereas the propagation term *P(f,R)* accounts for the effect of both the vertical variation of crustal impedance *Z(f)* and the amplitude attenuation with distance *R:*

$$P(f,R) = Z(f) \cdot D(f,R)\,. \qquad (2)$$

D(f,R) includes geometrical spreading and spectral attenuation. Further details are given in Boore (1983, 1986 a). According to Brune (1970), the source term in point-source approximation is expressed as

$$A_o(f) = \frac{F_S R_{\vartheta,\phi}}{4\pi\rho\beta^3} \frac{(2\pi f)^2 M_0}{1+(f/f_0)^2} \tag{3}$$

where F_S is a free-surface coefficient (2), $R_{\vartheta,\phi}$ is the station radiation pattern, ρ is the density and β the shear-wave velocity in the source volume. Following Chiarabba *et al.* (2005), we used 2.6 g/cm^3 and 3.2 km/s, respectively, for the latter two parameters. M_0 and f_0 are seismic moment and corner frequency, respectively. The M_0 estimates, 4.3 and 4.6 10^{24} dyne·cm respectively for the first and second mainshock, were taken from the MedNet catalogue (http://mednet.rm.ingv.it; see also Pondrelli *et al.*, 2004).

Single-station spectral ratios are a powerful tool to deconvolve propagation effects from signals and assess source scaling (Chael, 1987; Boore and Atkinson, 1989; Rovelli *et al.*, 1991; Hough, 1997). When two earthquakes having different magnitude M_1 and M_2 are recorded at the same station, the ratio between their spectra

$$\frac{V_{M1}(f)}{V_{M2}(f)} = \frac{A_{0,M1}(f)P(f,R)H(f)}{A_{0,M2}(f)P(f,R)H(f)} = \frac{M_{0,M1}}{M_{0,M2}} \cdot \frac{1+(f/f_{0,M2})^2}{1+(f/f_{0,M1})^2} \tag{4}$$

reduces to the ratio between the two source terms since crustal propagation and site terms are the same, provided that the distance between the hypocenters is small compared to the station distance and that the two shocks share the same source mechanism. In (4), the dependence of f_0 on M_0 and $\Delta\sigma$ is expressed by

$$\Delta\sigma = \frac{7}{16}\frac{M_0}{r^3} \tag{5}$$

and

$$r = \frac{2.34\beta}{2\pi f_0} \tag{6}$$

Therefore, Equation (4) is controlled by the ratio of the seismic moments at low frequency, and by the ratio of $M_0^{1/3}$ and $\Delta\sigma^{2/3}$ at high frequency. Since seismic moments are derived from independent

estimates, $\Delta\sigma$ is the only unknown parameter. The relationship between $\Delta\sigma$ and M_0 can be inferred through a best fit of the empirical spectral ratios over an extended magnitude range, assuming a power law of the type

$$\log \Delta\sigma = p \ \log M_0 \ + \ q. \tag{7}$$

The misfit is given by

$$\varepsilon^2 = \frac{\sum_{m=1,M} \ \sum_{n=N_1,N_2} (\log Obs_{m,n} - \log Theo_{m,n})^2}{M(N_2 - N_1)} \tag{8}$$

where $Obs_{m,n}$ are the empirical spectral ratios calculated from couples of events with different magnitudes and $Theo_{m,n}$ are the corresponding mathematical functions (4) that are written in terms of M_0, p, and q through (5), (6), and (7). The couple p and q that minimize (8) define the source scaling by means of (7). In (8), M is the number of the spectral ratios curves used in the fit; N_1 and N_2 are the indexes corresponding to f_{min} and f_{max}, i.e. the lower and upper bounds of the frequency band of analysis (0.2 and 10 Hz, respectively).

Using this strategy we bypassed the well known difficulties due to bandwidth limitation when source scaling is assessed through corner frequency (Boore, 1986 b; Di Bona and Rovelli, 1988). The first evident advantage of using (4) is that the mainshock corner frequency is not required to be inside the frequency band of analysis. The very requirement is that f_0 (of smallest aftershocks) must be lower than f_{max}, the amplitude spectra being insensitive to $\Delta\sigma$ below f_0. The minimum values of $\Delta\sigma$ found in this study (of the order of few bars) correspond to corner frequencies of about 4 Hz, well below f_{max}.

In the second method of analysis, we assessed source radiation spectra $A_0(f)$ of the mainshocks through the Fourier amplitude spectra $A(f)$ of the two horizontal components of processed accelerograms, according to Equations (1) and (2)

$$A_0(f) = \frac{A(f)}{D(f,R) \cdot Z(f) \cdot H(f)} \tag{9}$$

Time windowing and smoothing procedures were the same previously described for the broad-band seismogram analysis. Stress drop is then inferred from the flat level of the high-frequency acceleration plateau which, based on the assumption of the omega-square model, scales as $A_o(f) \approx$

$M_o\, f_o^2 \approx \Delta\sigma^{2/3}$, the explicit relationship being provided by (5) and (6). In (9), the amplification function due to the vertical impedance variation *Z(f)* was computed through the velocity model shown in Figure 4 (gray curve). This is essentially the 1D model proposed by Chiarabba *et al.* (2005) for P-wave velocity (α), with $\alpha / \beta = 1.9$, but we have replaced the uppermost uniform layer (β = 1.7 km/s) with a constant gradient layer where β varies from 3.1 km/s at the bottom interface to a conventional value of 800 m/s at the surface. This value is the lower bound of site class A as defined in CEN (2004). By doing so we adopted a realistic value of S-wave velocity for near-surface rocks, maintaining the travel times of the original model unchanged after the linear gradient modification. The velocity inversion at 12 km depth is the effect of the underthrusting of the Apulian platform beneath the Apennines (Chiarabba *et al*., 2005). Figure 4 shows a comparison of the crustal transfer function assessed for vertical incidence using the Haskell (1960) approach (the program RATTLE, courtesy by C. Mueller, U.S. Geological Survey) and the square-root impedance amplification function computed following Boore (1986 a). We have used the latter because of its more regular, smoothed behavior. To account for a realistic source-to-receiver geometry, the incidence angle was varied versus epicentral distance in a range from 45° at 30 km to 60° at 60 km for direct rays (stations GLD, CMM, SCV, VSE) and was fixed at 45° for refracted waves, beyond 100 km (stations RTU and ASSE).

The other propagation term in (9), *D(f,R)*, represents the effect of geometrical spreading and spectral attenuation. Different expressions of *D(f,R)* of central Italy taken from the literature (Castro *et al*., 1999; Malagnini *et al.*, 2000) were tentatively checked but resulted in unrealistic trends in the derived source spectra because of a significant overcorrection in the upper part of our frequency band of analysis. This was probably due to the different source depth ($12 \le h \le 20$ km) of the 2002 Molise earthquakes with respect to the shallower earthquakes ($h < 10$ km) used by Castro *et al.* (1999) and Malagnini *et al.* (2000) for estimating their attenuation models.

We then adopted the functional form

$$D(R, f) = \frac{\exp(-\pi\kappa f)}{R} \tag{10}$$

where $1/R$ is a spherical geometrical spreading term, κ is the integral along the source-to-receiver path *S* and *Q* is the crust quality factor (Anderson and Hough, 1986)

$$\kappa = \int_S \frac{ds}{\beta(s)Q(s)} \tag{11}$$

The parameter κ is computed for every station from the high-frequency acceleration spectral slope. With this choice we forced the source spectra to obey the omega-square model.

Finally, the site effect term was fixed a priori

$$H(f) = 1 \qquad (12)$$

having the near-site velocity structure been accounted for in the modified velocity profile of Figure 4. According to the ITACA data base (at: http://itaca.mi.ingv.it), we selected stations located on firm sites (CMM, SCV, GLD, VSE, RTU, ASSE); stations on soft sites (SNN, LSN, SSV, CHIE, AVZ, NOR) were consistently excluded from the analysis to prevent contamination of the inferred source spectra by local site effects.

Spectral scaling from broad-band velocity-sensor records

The strong-motion accelerographs that recorded the mainshocks were not triggered by small magnitude aftershocks, and only the three seismological stations AQU, CII, and ARC1 recorded the entire sequence including the two mainshocks. ARC1 is especially suitable because, due to its location (about 60 km south of the epicentral area), it falls in the maximum of the radiation pattern for SH waves and is unaffected by possible directivity effects that could bias the stress drop estimate when a single station is used. The site geology was chosen by Improta *et al.* (2005) to be as much as possible representative of the bedrock reference motion in their microzoning study. The dataset is especially valuable also because its signal-to-noise ratio is >3 in the frequency band 0.2-10 Hz even for aftershocks as small as M_W 2.7. Although the seismograms of the two mainshocks were digitally clipped around ±0.25 cm/s, the clipping affected mostly low-frequency peaks after the direct body wave trains (see details in the Appendix A). We have artificially clipped the velocity time history of a nearby accelerometric station (SCV), reproducing on the SCV record the same duration of the saturated portion of ARC1. In Appendix A we compare the Fourier spectra of real and artificially saturated data of SCV; this allows us to infer that the effect of clipping on spectral amplitudes is an underestimation of less than 20%, on average, limitedly to the lowest part of the frequency band of analysis. We conclude that the effect of clipping is minimum compared to other parameter uncertainties and can be neglected in spectral estimates.

We then used the records of ARC1 for the source scaling analysis. Table 1 lists 14 aftershocks that were selected on the basis of a satisfactory waveform consistency with the mainshocks. For the sake of example, particle motions of large and small events are shown in the upper panels of Figure 5. Selected events fall in the M_0 range

$$1.4\ 10^{20} \leq M_0 \leq 4.6\ 10^{24}\ \text{dyne·cm.} \qquad (13)$$

The seismic moment of aftershocks was estimated from the low-frequency spectral amplitude (Ω_0) of horizontal source ground displacement $\Omega(f)$

$$\Omega_0 = \frac{F_S R_{\vartheta,\phi}}{4\pi\rho\beta^3}\frac{M_0}{R} \qquad (14)$$

where, recalling (1) and (2), ground displacement $\Omega(f)$ is written as

$$\Omega(f) = \frac{A_0(f)}{(2\pi f)^2}\cdot P(f,R) \qquad (15)$$

According to Equation (2), $P(f,R)$ includes the geometrical spreading $1/R$, the spectral attenuation correction (κ=0.099 s), and the crust impedance term $Z(f)$. The latter was computed through the velocity profile and source depth (20 km) taken from Chiarabba *et al.* (2005), using a 60° incidence angle (see Figure 4, full smooth curve). All spectra were scaled to a distance of 60 km.

The M_0 and M_w values of the selected aftershocks are listed in Table 1; moment-magnitudes M_w were computed from M_0 following Hanks and Kanamori (1979)

$$\log M_0 = 1.5M_w + 16.1 \qquad (16)$$

To achieve a higher stability in the spectral ratio computation, we used an average spectrum of the smallest four aftershocks (#2, 4, 5, and 10 in Table 1) in the denominator. Their seismic moments fall in the range $1.4 \leq M_0 \leq 3.5\ 10^{20}$ dyne·cm and their geometric mean is $2.3\ 10^{20}$ dyne·cm (M_w 2.8).

Figure 5c shows the trend of the spectral ratios at different magnitudes, displaying a regularly scaled behavior in the spanned magnitude range. Concerning the two basic assumptions of the spectral ratio method (same hypocenter and same source mechanism), we remark that the distance between the hypocentral coordinates is in the range 3 to 10 kms, within the size of the ruptured fault planes (Vallée and Di Luccio, 2005) and much smaller than the source-to-receiver distance. The control on the source mechanism was made by checking horizontal particle motion

(see Figure 5, a and b). Although this check is only qualitative and somewhat disturbed by a strong P-to-S conversion at the top of the Apulia Carbonate Platform (Latorre *et al.*, 2008), mainshocks and selected aftershocks are enough well correlated in the frequency domain (see Figure 5 d). Nevertheless we also applied the best fit (8) to Fourier amplitude spectra of ARC1, an approach that does not require any constraint on the hypocenter and focal mechanism, and found very consistent results (see Appendix B).

We used a trial-and-error approach-to search for the couple (p, q) that minimizes the variance of misfit between observed and theoretical spectral ratios according to (7) and (8), using a discretized grid ranging in the intervals

$$0.00 \leq p \leq 0.60 \qquad -10.0 \leq q \leq 0.0 \tag{17}$$

with increments of $\Delta p = 0.01$ and $\Delta q = 0.1$. The method resolution can be evaluated in Figure A2, panel a (Appendix B). Only the spectral ratios between the two mainshocks and the reference spectrum were used in the fit because spectral fluctuations mask the minimum of the variance misfit when the magnitude difference between the numerator and the denominator is small. The least-mean-square solution (minimum misfit ε equal to 0.026) is found when

$$p = 0.15$$
$$q = -2.8 \tag{18}$$

This solution yields

$$\Delta\sigma = 8 \text{ bars at } M_w = 5.7$$
$$\Delta\sigma = 2 \text{ bars at } M_w = 2.7 \tag{19}$$

Figure 5c shows a comparison between the observed spectral ratios and the best-fit theoretical trend (full gray lines). Although only the two mainshocks were used in the fit, spectral ratios of all the events of Table 1 are fairly well matched by the inferred scaling (19). The two mainshock spectral ratios are also compared with the curve (dotted line) that minimizes the misfit ($\varepsilon = 0.040$) when a constant stress drop scaling is assumed. In this case, the best fit is found at $\Delta\sigma = 25$ bars. This fit overestimates the spectral ratios at low frequency and underestimates them at high frequencies. However, both constant and varying stress drop curves indicate a low stress drop scaling. We have also drawn the trend of the MM08 source scaling, that attributes 180 bars to the

31 October mainshock with an uncertainty range of 45 to 717 bars, and 20 bars to the magnitude of the reference aftershock, with an uncertainty range of 18 to 22 bars. Although quite wide, the uncertainty band of MM08 (shaded in Figure 5) does not match the observations, intercepting only partially their trend at very high frequency. For a consistency check, Figure 5d shows a comparison between absolute ground motion amplitudes of ARC1 with the stress drop scaling given by (19). Theoretical spectra are attenuated according to (9), with the velocity impedance function *Z(f)* computed from the 1-D crustal model for an incidence angle of 60°. In applying (9), *H(f)* has been put equal to 1, the near-site impedance variation having been included in the modified velocity profile of Figure 4.

Figure 5d confirms the validity of the spectral ratio scaling (19) also in terms of absolute ground motion amplitudes. Appendix B shows the results of an independent best fit using the acceleration spectra of Figure 5d instead of the spectral ratios of Figure 5c. The very consistent fit of spectral ratios and absolute amplitudes, that are based on different equations, suggests i) that the inferred source scaling is stable even though the basic assumptions for the applicability of spectral ratios, i.e. that the hypocenter and the source mechanism are the same, cannot be strictly proved, and ii) that propagation is correctly modeled .

Finally, we checked the spectral ratios of AQU and CII. We searched for aftershocks that were used by MM08 and are also included in Table 1. There is only one event at both AQU and CII that was also used in the ARC1 analysis (# 7, M_W 3.7). Figure 6 shows the comparison between the spectral ratios of ARC1, AQU, and CII for this earthquake. The three stations look very similar in terms of spectral ratios, although individual spectra show large fluctuations (Figure 7). Using the high stress drops proposed by MM08 (180 and 170 bars respectively for the 31 October and 1 November events), makes it impossible to fit single-station spectral ratios of all three stations. In contrast, the two curves based on smaller values of stress drop are much more consistent with the data shown in Figure 6: at low frequency (f < 2 Hz) a better agreement is achieved using (19), whereas at high frequency the 25-bars constant stress drop scaling works better (thin black line and thick gray line, respectively). Also the absolute amplitudes of the mainshocks are not fit by the MM08 stress drops (dashed curves in Figure 7), the misfit of AQU and CII being significant. For the aftershock of Figure 7, ARC1 shows large spectral fluctuations in terms of absolute amplitudes, but low and high frequencies are well fit by our prediction of 3 bars according to (19). In contrast, the aftershock amplitude spectra of AQU and CII seem to be better fit by the MM08 scaling (38 bars), but their deviation from the theoretical spectra computed according to the scaling law (19) (full curve) is similar to that of the mainshocks, suggesting that this deviation could be due to a propagation effect.

Spectra of strong-motion accelerograms

The high-frequency strength of the incident seismic radiation is characterized by the parameters κ and Δσ. They have a competing role in controlling the high-frequency ground motion, with a strong tradeoff (Boore *et al.*, 1992). The former parameter (see Eq. 11) was defined by Anderson and Hough (1984) and is estimated through the slope of the spectral decay of ground acceleration, under the assumption that *Q* is frequency-independent. The latter (Δσ) controls the level of ground acceleration according to Equations (3), (5), and (6).

We first computed κ for all accelerometric stations through the conventional technique based on the estimate of the spectral decay of ground acceleration in a log-lin plot (first applied by Anderson and Hough, 1984). An average κ for each station is obtained from the geometric mean of the four spectra deriving from the two horizontal components for the two mainshocks (Figure 8, top panels). The statistical uncertainty (error bars in the bottom panel) is estimated as the minimum and maximum slope of the linear regression. The results indicate that the κ values found in this study for stiff and soft sites are not larger than those found by Rovelli *et al.* (1988) (hereinafter R88), who investigated attenuation and scaling laws of ground motion in the Apennines during weak- to moderate-magnitude normal faulting earthquakes. Even though the number of observations is different for the two datasets and they are both quite dispersed, the results of Figure 8 provide a first, rough indication that there is no evidence for a higher source-to-station spectral attenuation in the records of the Molise earthquakes compared to other Apennines earthquakes. This confirms that a low stress drop is a viable explanation for the observed weak shaking.

Therefore, we reconstructed the source-radiated acceleration spectrum $A_0(f)$ of the two Molise mainshocks correcting observed spectra $A(f)$ for the propagation effects. Observed spectra are shown in Figure 9 (a and b). According to Equation (9), these spectra were scaled to a reference distance of 1 km through $D(f,R)$, and then the crustal impedance correction $Z(f)$ was applied. As shown in Figure 4, the latter was computed for different incidence angles depending on the station distance. The spectra were also corrected for the conventional radiation pattern coefficient (0.63). Our final results for the source-radiated acceleration spectra are shown in Figures 9c and 9d for the 31 October and 1 November shocks, respectively.

The bottom panels of Figure 9 bring a further argument in favor of a low stress drop of Molise earthquakes: all rock stations are significantly below the MM08 estimates. The high-frequency acceleration plateaus of Figures 9c and 9d yield mean values of 16 and 12 bars for the 31 October and 1 November shocks, respectively, the intervals of statistical uncertainty (±1 s.d. around the geometric mean, shadowed in Figure 9) being equal to 9-26 and 8-19 bars.

The conclusion emerging from Figure 9 (c and d) is that our reconstruction of source-radiated accelerations, that takes into account the velocity inversion, confirms the low stress drops inferred from spectral ratios and Fourier amplitudes of broad-band seismograms recorded at ARC1. The source spectra of accelerograms are consistent with small stress drops of about 20 bars.

Finally, in order to assess to what extent the tradeoff between κ and $\Delta\sigma$ (Boore *et al.*, 1992; Sonley and Abercrombie, 2006) could have affected the stress drop estimates inferred from the high-frequency plateu of Figure 9, we overcompensated the propagation correction using κ + 1 s.d. instead of κ. We obtained stress drop values that increase by about 15% for each station, leaving our conclusions unchanged.

Discussion and conclusions

Seismological analyses (Vallée and Di Luccio, 2005, and this study) and geodetic observations (Giuliani *et al.*, 2007) provide strong evidence for a small stress drop in the 2002 Molise earthquakes. According to Calderoni *et al*. (2009), it is 3 to 4 times smaller than that typical of similarly large normal faulting Apennines earthquakes. Preliminary results from spectral ratios of the recent April 2009, L'Aquila earthquakes also yield a stress drop of the order of 50 bars for the M_W 6.3 mainshock. The low stress drop found in this study is unusual for Apennines earthquakes but not isolated: the 5 May 1990, Potenza earthquake (M_w 5.8) also supplied evidence for a long source duration, that Ekström (1994) ascribed to a low stress drop. The 1990 and 2002 earthquake sequences share similar source mechanisms, as they were both generated by right-lateral slip on relatively deep (from 12 to 25 km) fault planes, and a similar tectonic framework. Both sequences had a similar magnitude mainshock and were swarm-like (the 1990 Potenza sequence extended for over a year culminating with another M_w 5.2 shock on 26 May 1991). A similar focal mechanism is reported by Gasparini *et al.* (1985) for the 6 May 1971, M_L 4.9, Monteleone di Puglia and by Riguzzi (1999) for the 19 June 1975, M_L 4.8, Gargano earthquakes (see Figure 12), all of which occurred within the Apulian foreland.

Based on evidence from all these earthquakes, Valensise *et al.* (2004) argued that the current state of stress of the Apennines lithosphere is different at different crustal levels. In particular, the stress field associated with the 2002 Molise earthquakes is very different - though kinematically compatible - from the stress field that controls the NE-SW extension along the crest of the Apennines (in both cases the minimum stress axis is oriented northeast). Valensise *et al.* (2004) contended that the Apennines comprise a multi-story edifice: the upper level is characterized by the extension-compression pair associated with the build-up of the accretionary prism, whereas the lower level is dominated by the compressional stress field that accompanies the deformation of the

subducted complex. This slant plate is partly exposed in the Gargano promontory, where its kinematics have already been unveiled, but is found at 10-25 Km depth below the southern Apennines. Seismicity in the lower level is due to large-scale reactivation of pre-existing lines of weakness within the subducted complex, more specifically a suite of regional E-W strike-slip shear zones (Di Bucci *et al.*, 2006; Fracassi and Valensise, 2007). These faults, that were generated as left-lateral during the construction of the chain, are now being used as right-lateral under the current stress conditions.

What caused the low-stress drop observed in the 1990 and 2002 earthquakes? Based on the tectonic history of the region we may speculate that the seismicity of the E-W shear zones is a result of the roughness of the two sides of faults slipping past each other with a sense opposite to that characterizing their earlier phases. This could cause a weaker release of energy due to re-rupturing mechanisms in lower friction conditions on these faults. Notice that in other regions of the world low stress drop earthquakes are normally interpreted as the result of re-rupturing after short healing times (Kanamori *et al.*, 1993; Berberian *et al.*, 1999); but this circumstance hardly applies to the southern Apennines and to Molise-type earthquakes in particular, since local strain rates are relatively small and typical repeat times are in the order of 2,000 years or more (see Basili *et al.*, 2008, for a summary).

Our hypothesis implies that the low stress drop detected in the 2002 earthquakes is a permanent characteristic of a set of seismogenic sources lying in this portion of the Italian peninsula. Although anomalously low-energetic sources have been observed instrumentally only for the 1990 Potenza and 2002 Molise earthquakes, it is very likely that similar source properties are shared by several other historical earthquakes, starting with the multiple shocks forming the 5-30 December 1456 sequence, the largest concentration of seismic moment release in Italian history (Fracassi and Valensise, 2007). The new seismic hazard zonation of Italy (Meletti *et al.*, 2008) also acknowledges the existence of such deeper sources. The peculiar source characteristics of earthquakes of this class may have a profound impact on the calculation of the associated seismic hazard, especially in the context of assessing the true magnitude of historical events and predicting the ground shaking for future ones.

Acknowledgments

We wish to thank Joe Fletcher, an anonymous reviewer, and the Associate Editor Michel Bouchon for many critical comments and very constructive suggestions. We also benefited of many discussions and a thorough revision by Dave Boore, which led to a substantial improvement of the manuscript. Daniela Riposati skillfully prepared most of the figures. This paper benefited from data

and financial support from the Traiano Project of the Gruppo Nazionale Difesa dai Terremoti (2000-2003) and from the project "Ground shaking and expected damage scenarios in prioritiy and/or strategic areas" developed within the 2004-2006 agreement between INGV and the Italian Department of Civil Protection.

References

Allmann, B. P., and P. M. Shearer (2009). Global variations of stress drop for moderate to earthquakes, *J. Geophys. Res*., **114**, B01310, doi:10.1029/2008JB005821.

Anderson, J. G. and S. E. Hough (1984). A model for the shape of the Fourier amplitude spectrum of acceleration at high frequencies, *Bull. Seism. Soc. Am*., **74**, 5, 1969-1993.

Basili, R., G. Valensise, P. Vannoli, P. Burrato, U. Fracassi, S. Mariano, M. M. Tiberti, and E. Boschi (2008). The Database of Individual Seismogenic Sources (DISS), version 3: summarizing 20 years of research on Italy's earthquake geology, *Tectonophysics*, **447**, doi:10.1016/j.tecto.2007.04.014.

Berberian, M., J. A. Jackson, M. Qorashi, M. M. Khatib, K. Priestley, M. Talebian, and M. Ghafuri-Ashtiani (1999). The 1997 May 10 Zirkuh (Qa'enat) earthquake (Mw 7.2): faulting along the Sistan suture zone of eastern Iran, *Geophys. J. Int.*, **136**, 3, 671-694.

Bindi, D., L. Luzi, and F. Pacor (2009). Inter-event and inter-station variability computed for the Italian Accelerometric Archive (ITACA), *Bull. Seism. Soc. Am*. (in press).

Boore, D. M. (1983). Stochastic simulation of high-frequency ground motions based on seismological models of the radiated spectra, *Bull. Seism. Soc. Am*., **73**, 1865-1894.

Boore, D. M. (1986 a). Short-period P- and S-wave radiation from large earthquakes: implications for spectral scaling relations, *Bull. Seism. Soc. Am*., **76**, 43-64.

Boore, D. M. (1986 b). The effect of finite bandwidth on seismic scaling relationships, in *Earthquake Source Mechanics*, S. Das, J. Boatwright, and C.H. Scholz, Editors, *A.G.U. Monograph 37*, 275-283.

Boore, D. M. and G. M. Atkinson (1989). Spectral scaling of the 1985 to 1988 Nahanni, Northwest Territories, earthquakes, *Bull. Seism. Soc. Am*., **79**, 1736-1761.

Boore, D. M., W. B. Joyner, and L. Wennerberg (1992). Fitting the stochastic ω^{-2} source model to observed response spectra in western North America: trade-offs between $\Delta\sigma$ and κ, *Bull. Seism. Soc. Am.*, **82**, 1956-1963.

Boore, D. M., W. B. Joyner, and T. E. Fumal (1997). Equations for estimating horizontal response spectra and peak acceleration from western North American earthquakes: A summary of recent work (with 2005 erratum), *Seism. Res. Lett.*, **68**, 128-153.

Boore, D. M, C. D. Stephens, W. B. Joyner (2002). Comment on baseline correction of digital strong-motion data: examples from the 1999 Hector Mine, California, earthquake, *Bull. Seism. Soc. Am.*, **92**, 1543–1560.

Boore, D. M. and J. J. Bommer (2005). Processing of strong-motion accelerograms: needs, options and consequences, *Soil Dyn. Earthq. Eng.*, **25**, 93-115.

Brune, J. N. (1970). Tectonic stress and the spectra of seismic shear waves from earthquakes, *J. Geophys. Res.*, **75**, 4997-5009 (and Errata, *J. Geophys. Res.*, **76**, 5002, 1971).

Calderoni, G., A. Rovelli, G. Milana, and G. Valensise (2009). What is the stress drop of mid-size Apennines earthquakes? *Seism. Res. Lett.*, **80**, 336-337 (abstract).

Cara, F., A. Rovelli, G. Di Giulio, F. Marra, T. Braun, G. Cultrera, R. Azzara, and E. Boschi (2005). The role of site effects on the intensity anomaly of San Giuliano di Puglia inferred from aftershocks of the Molise, Central Southern Italy, sequence, November 2002, *Bull. Seism. Soc. Am.*, **95**, 1457-1468.

Castro, R. R., G. Monachesi, M. Mucciarelli, L. Trojani, and F. Pacor (1999). P- and S-wave attenuation in the region of Marche, Italy, *Tectonophysics*, **302**, 123–132.

CEN, European Committee for Standardization (2004). Eurocode 8: design of structures for earthquake resistance - Part 1: general rules, seismic actions and rules for buildings. Bruxelles, Belgium.

Chael, E.P. (1987). Spectral scaling of earthquakes in the Miramichi region of New Brunswik, *Bull. Seism. Soc. Am.*, **77**, 347-365.

Chiarabba, C., P. De Gori, L. Chiaraluce, P. Bordoni, M. Cattaneo, M. De Martin, A. Frepoli, A. Michelini, A. Monachesi, M. Moretti, G. P. Augliera, E. D'Alema, M. Frapiccini, A. Gassi, S. Marzorati, P. Di Bartolomeo, S. Gentile, A. Govoni, L. Lovisa, M. Romanelli, G. Ferretti, M. Pasta, D. Spallarossa, and E. Zumino (2005). Mainshocks and aftershocks of the 2002 Molise seismic sequence, southern Italy, *J. Seismol*., **9**, 487-494.

Cocco, M., and A. Rovelli (1989). Evidence for the variation of stress drop between normal and thrust faulting earthquakes in Italy, *J. Geophys. Res.*, **94**, B7, 9399-9416.

De Martini, P. M., N. A. Pino, G. Valensise, and S. Mazza (2003). Geodetic and seismologic evidence for slip variability along a blind normal fault in the Umbria-Marche 1997–1998 earthquakes (central Italy), *Geophys. J. Int.*, **155**, 3, 819–829, doi:10.1111/j.1365-246X.2003.02049.x.

Di Alessandro, C., F. Bonilla, A. Rovelli, and O. Scotti (2008). Influence of site classification on computing empirical ground-motion prediction equations in Italy, *EOS Trans. Am. Geophys. Un*., **89**, 53, *Fall Meet. Suppl.*, Abstract S12A-05.

Di Bona, M., and A. Rovelli (1988). Effects of the bandwidth limitation on stress drops estimated from integrals of the ground motion, *Bull. Seism. Soc. Am.*, **78**, 1818-1825.

Di Bucci, D., A. Ravaglia, S. Seno, G. Toscani, U. Fracassi, and G. Valensise (2006). Seismotectonics of the southern Apennines and Adriatic foreland: insights on active regional E-W shear zones from analogue modelling, *Tectonics*, **25**, 4, TC4015, doi: 10.1029/ 2005TC001898.

Di Giulio, G., L. Improta, G. Calderoni, and A. Rovelli (2008). A study of the seismic response of the city of Benevento (southern Italy) through a combined analysis of seismological and geological data, *Engineering Geology*, **97**, 146-170, doi: 10.1016/j.enggeo.2007.12.010.

DISS Working Group, Database of Individual Seismogenic Sources (2007), Version 3.0.3: A compilation of potential sources for earthquakes larger than M 5.5 in Italy and surrounding areas, http://www.ingv.it/DISS/, © INGV 2005.

Dolce, M., A. Masi, C. Samela, G. Santarsiero, M. Vona, G. Zuccaro, F. Cacace, and F. Papa (2004). Esame delle caratteristiche tipologiche e del danneggiamento del patrimonio edilizio di San Giuliano di Puglia, *XI Congresso Nazionale "L'ingegneria Sismica in Italia"*, 25-29 January 2004, Genova, Italy (in Italian).

Ekström, G. (1994). Teleseismic analysis of the 1990 and 1991 earthquakes near Potenza, *Ann. Geophys.*, **37**, 1591-1599.

Fracassi, U. and G. Valensise (2007). Unveiling the sources of the catastrophic 1456 multiple earthquake: Hints to an unexplored tectonic mechanism in southern Italy, *Bull. Seism. Soc. Am.*, **97**, 3, 725-748, doi:10.1785/0120050250.

Galli, P. and D. Molin (2004). Macroseismic survey of the 2002 Molise, Italy, earthquake and historical seismicity of San Giuliano di Puglia, *Earthquake Spectra*, **20**, *S1*, S39–S52, doi:10.1193/1.1766034.

Gasparini, C., G. Iannaccone, and R. Scarpa (1985). Fault-plane solutions and seismicity of the Italian peninsula, *Tectonophysics*, **117**, 59-78.

Giuliani, R., M. Anzidei, L. Bonci, S. Calcaterra, N. D'Agostino, M. Mattone, G. Pietrantonio, F. Riguzzi, and G. Selvaggi (2007). Co-seismic displacements associated to the Molise (Southern Italy) earthquake sequence of October–November 2002 inferred from GPS measurements. *Tectonophysics*, **432**, 21–35, doi:10.1016/j.tecto.2006.11.005.

Gorini, A., S. Marcucci, P. Marsan, and G. Milana (2004). Strong motion records of the 2002 Molise, Italy, earthquake sequence and stochastic simulation of the main shock, *Earthquake Spectra*, **20**, *S1*, S65-S79.

Goretti, A. (2006). Spatial cluster analysis and site effects in San Giuliano based on building typology and damage data collected after the 2002 Molise earthquake. *Boll. Geof. Teor. Appl.*, **47**, 39-52.

Hanks, T. C., and H. Kanamori (1979). A moment magnitude scale, *J. Geophys. Res.*, **84**, B5, 2348-2350.

Hanks, T. C., and D. M. Boore (1984). Moment-magnitude relations in theory and practice, *J. Geophys. Res.* **89**, 6229-6235.

Haskell, N. A. (1960). Crustal reflection of plane SH waves, *J. Geophys. Res.*, **65**, 12, 4147-4150.

Hough, S.E. (1997). Empirical Green's function analysis: taking the next step, *J. Geophys. Res.*, **102**, B3, 5369-5384.

Kanamori, H., J. Mori, E. Hauksson, T. H. Heaton, L. K. Hutton, and L. M. Jones (1993). Determination of earthquake energy release and M_L using Terrascope, *Bull. Seism. Soc. Am.*, **83**, 330-346.

Improta, L., G. Di Giulio, and A. Rovelli (2005). Variations of local seismic response in Benevento (southern Italy) using earthquakes and ambient noise recordings, *J. Seismol.*, **9**, 191-210.

Latorre, D., P. De Gori, C. Chiarabba, A. Amato, J. Virieux, and T. Monfret (2008). Three-dimensional kinematic depth migration of converted waves: application to the 2002 Molise aftershock sequence (southern Italy), *Geophysical Prospecting*, **56**, 587-600 doi:10.1111/j.1365-2478.2008.00711.x.

Maffei, J. and P. Bazzurro (2004). The 2002 Molise, Italy, Earthquake, *Earthquake Spectra*, **20**, S1-S22, doi:10.1193 /1.1770976.

Malagnini, L., R. Herrmann, and M. Di Bona (2000). Ground-motion scaling in the Apennines (Italy), *Bull. Seism. Soc. Am.*, **90**, 1062-1081.

Malagnini, L., and K. Mayeda (2008). High-stress strike-slip faults in the Apennines: an example from the 2002 San Giuliano earthquakes (Southern Italy), *Geophys. Res. Lett.*, **35**, doi:10.1029/2008GL034024.

Mazza, S., M. Olivieri, A. Mandiello, and P. Casale (2008). The Mediterranean Broad Band Seismographic Network Anno 2005-2006. In: *Earthquake Monitoring and Seismic Hazard Mitigation in Balkan Countries*, E. S. Husebye (ed.), NATO Science Series: IV: Earth and Environmental Sciences, Vol. 81, XVIII, 289 pp., with CD-ROM, Springer Science+Business Media B.V. 2008.

Meletti, C., F. Galadini, G. Valensise, M. Stucchi, R. Basili, S. Barba, G. Vannucci, and E. Boschi (2008). The ZS9 seismic source model for the seismic hazard assessment of the Italian territory, *Tectonophysics*, **450**, 85-108, doi: 10.1016/j.tecto.2008.01.003.

Paolucci, R., A. Rovelli, E. Faccioli, C. Cauzzi, D. Finazzi, M. Vanini, C. Di Alessandro, and G. Calderoni (2008). On the reliability of long-period response spectral ordinates from digital accelerograms, *Earthquake Engng Struct. Dyn.*, **37**, 697–710, doi: 10.1002/eqe.781.

Pondrelli S., A. Morelli, and G. Ekström (2004). European-Mediterranean Regional Centroid Moment Tensor catalog: solutions for years 2001 and 2002, *Phys. Earth Planet. Int.*, **145**, 1-4, 127-147.

Riguzzi, F. (1999). Intensity Field of the 19 June 1975 Gargano (Southern Italy), earthquake, *Phys. Chem. Earth*, Part A *24*, 489-493.

Rovelli, A., O. Bonamassa, M. Cocco, M. Di Bona, and S. Mazza (1988). Scaling laws and spectral parameters of the ground motion in active extensional areas in Italy, *Bull. Seism. Soc. Am.*, ***78***, 530-560.

Sabetta, F., and A. Pugliese, (1987). Attenuation of peak horizontal acceleration and velocity from Italian strong-motion records, *Bull. Seism. Soc. Am.*, ***77***, 1491-1513.

Sonley, E., and R. E. Abercrombie (2006). Variability in source parameters, as measured downhole at Parkfield, CA, *Seism. Res. Lett.,* **77,** 256**.**

Valensise, G., D. Pantosti, and R. Basili (2004). Seismology and Tectonic Setting of the 2002 Molise, Italy, Earthquake, *Earthquake Spectra*, **20**, S23-S37, doi:10.1193/1.1756136.

Vallée, M. and F. Di Luccio (2005). Source analysis of the 2002 Molise, southern Italy, twin earthquakes (10/31 and 11/01), *Geoph. Res. Lett.*, **32**, L12309, doi:10.1029/2005GL022687.

Working Group ITACA (2008). Database of the Italian strong-motion data. Available from: http://itaca.mi.ingv.it.

Appendix A

ESTIMATE OF SPECTRAL DEPLETION DUE TO CLIPPING

The twin M_W 5.7 Molise earthquakes of 31 October and 1 November 2002 provided clipped seismograms at 8 seismological stations operating in the town of Benevento, about 60 km south of the epicenters. These stations had been installed in 1999 for a microzoning experiment in the framework of the TRAIANO Project (Improta *et al.*, 2005). Clipping caused saturation of the horizontal components at an amplitude of ±0.25 cm/s, and the duration of the clipped seismogram portions varied among stations depending on the local site conditions. The reference station during the experiment (ARC1) suffered the lowest clipping effect, mostly in later arrivals (see Figure A1). ARC1 recorded the aftershocks on-scale and these data are ideal for a source scaling study, provided that the distortion due to clipping does not affect the mainshock waveforms below the saturation threshold and that the amplitude underestimation is demonstrated to be negligible.

The availability of a strong-motion accelerogram at San Marco dei Cavoti (SCV), a stiff-site station about 20 km north of Benevento along the same source backazimuth, makes the estimate of the clipping effect feasible. The spectral content of ARC1 and SCV is similar. Therefore, the velocity time series derived from the accelerograms of SCV are compared to the ARC1 records both in terms of amplitude and shape of the waveforms (Figure A1). This comparison suggests that instrumental response stayed linear at ARC1, and that the waveforms below the threshold did not suffer a significant distortion. Amplitudes of the horizontal components of SCV were scaled to the epicentral distance of ARC1 and artificially clipped at ±0.25 cm/s. This resulted in a total duration of 14.6 s for the clipped waveform portions of the two horizontal components, comparable (less than a factor of two difference) to that of ARC1. Therefore, we further scaled the SCV amplitude to get the same clipping duration at the two stations. The saturation threshold at SCV that gives the same duration of the clipped portions of ARC1 is 0.22 cm/s. The real recording of ARC1 and the velocity time series of SCV after clipping at 0.22 cm/s are shown in Figure A1. If we compare the spectra of observed and artificially clipped waveforms of SCV (Figure A1) we find that the amplitude underestimation due to clipping rarely exceeds 20%. The effect of clipping is distributed quite uniformly in the frequency band 0-5 Hz, and tends to disappear for $f > 5$ Hz.

The simulation of clipping on SCV ground velocity allows us to conclude that the underestimation of spectral amplitudes due to clipping is small and can be neglected. ARC1 seismograms can therefore be confidently used for the source scaling analysis for the entire earthquake sequence.

Appendix B

SOURCE SCALING OF ACCELERATION AMPLITUDE SPECTRA AT ARC1

As noted by Boore and Atkinson (1989), only the simultaneous analysis of both ground motion amplitudes and spectral ratios can prevent errors arising from inadequate propagation corrections and unrealistic validity conditions for the spectral ratio application (i.e. that the hypocenter and focal mechanism of the target event and the aftershock must be similar). As a consistency check of the scaling law (19) inferred from single-station spectral ratios, we have also searched for the best fit of the acceleration spectra of mainshocks and aftershocks at ARC1 (shown in Figure 5d). We adopted the same functional dependence of $\Delta\sigma$ versus M_0 as done for spectral ratios (7); in this case, $Obs_{m,n}$ and $Theo_{m,n}$ (both plotted in Figure 5d) are respectively the Fourier amplitude spectra of recorded ground acceleration and the theoretical curves of the omega-square source model (2) attenuated according to (7).

The grid search was made over all the analyzed earthquakes (M = 16 in Eq. 7), with the same intervals of p and q as in (17) and the same increments $\Delta p = 0.01$ and $\Delta q = 0.1$. Also the frequency band of analysis is unchanged.

The least-mean-square solution is found for

$$p = 0.13$$
$$q = -2.4 \qquad (20)$$

that yields

$$\Delta\sigma = 6 \text{ bars at Mw} = 5.7$$
$$\Delta\sigma = 2 \text{ bars at Mw} = 2.7 \qquad (21)$$

This best fit solution is very close to that inferred from spectral ratios (19). Figure A2 compares the pattern of the variance misfit using spectral ratios (top panel) and Fourier acceleration amplitudes (bottom panel). This comparison suggests that spectral ratios have a significantly higher sensitivity in determining the best fit in terms of $\Delta\sigma$, indicating an extremely low reliability for high values of stress drop.

According to Boore and Atkinson (1989), the combined use of spectral ratios and absolute amplitudes of records appears to be a very efficient tool in source scaling studies. The former have the advantage of being independent of propagation models but require independent seismic moment

estimates and the two strict conditions of same hypocenter and same source mechanism, both difficult to be checked *a priori*; the latter can be strongly contaminated by the use of attenuation models. The finding of a very stable source scaling in (19) and (21) comprises a double, *a posteriori* guarantee that spectral ratios are applicable to our case and attenuation is correctly modeled.

Table Caption

Table 1 – Earthquakes considered in this study.

Figure Captions

Figure 1 – Schematic map of the study area, including the two mainshock epicenters (indicated by stars) and location of the available recording stations. An accelerograph (NOR) was located about 200 km northwest of the epicenters and is not shown in figure. Focal mechanisms of the mainshocks are from Pondrelli *et al.* (2004); the VI and VII MCS intensity isoseismals are redrawn from Galli and Molin (2004).

Figure 2 – Peak ground accelerations recorded during the two Molise mainshocks. Both stiff and soft sites tend to lie significantly below the Sabetta and Pugliese (1987) regression curves (solid and dashed black lines indicate stiff and soft soil, respectively). Predictive equations by Boore *et al.* (1997), specifically computed for strike-slip earthquakes, overestimate observations as well (gray curves). Three untriggered stations (TRV, BOI, STG) are also shown at their own epicentral distance: their trigger threshold on the vertical component was 10 gals (straight horizontal line).

Figure 3 - Time series (displacement, velocity and acceleration of the EW components, respectively from top to bottom) of four selected stations that recorded the 31 October mainshock. CMM, SCV and RTU are digital accelerographs (Kinemetrics Etna data logger and Episensor), whereas ARC1 was equipped with a Lennartz 3D-5s digital seismometer connected to a Marslite data logger. Notice the partial clipping effect at ARC1 in the velocity time series (see text for discussion).

Figure 4 - (Upper panel) Vertical profiles of the adopted Molise velocity model. P- and S-waves are distinguished by gray and black lines, respectively. The original profiles (full lines) by Chiarabba *et al*. (2005) are modified with a regular gradient (dashed lines) to yield a shear velocity of 800 m/s at the surface. (Lower panel) The 1D crustal transfer function of SH waves for vertical incidence (0°) in an Haskell approach is compared with the square-root impedance amplification function for the same incidence (dashed curve) computed as in Boore (1986 a). The other smooth

curve (solid line) is the square-root impedance amplification function estimated for an oblique incidence of 60°.

Figure 5 – Particle motions in the horizontal plane during (a) the 31 October 2002 mainshock, and (b) low-magnitude aftershock (# 10). (c) Single-station (ARC1) spectral ratios of the Molise sequence ($2.7 \leq M_w \leq 5.7$). The best fit curves (full lines) are relative to the increasing stress drop scaling (Eq. 18). Spectral ratios of the two mainshocks are also fit using $\Delta\sigma$=25 bars, which is the best fit value under the assumption of constant stress drop scaling (dotted curve). The shadowed band corresponds to the ± 1 s.d. uncertainties of Malagnini and Mayeda (2008) for the 31 October mainshock. (d) Scaling of ground acceleration spectra at ARC1, theoretical curves are drawn according to (21).

Figure 6 – Comparison of spectral ratios of ARC1, AQU, and CII. Amplitude spectra of the two mainshocks (31 October and 1 November on the left and right panel, respectively) are divided by the spectrum of one aftershock (#7 of Table 1) available at the three stations. Theoretical curves are: (thin black line) scaling (Eq.19), (full gray line) constant stress drop scaling of 25 bars, (shadowed band) ±1 s.d. uncertainties of the stress drop scaling proposed by MM08.

Figure 7 – Observed spectra at ARC1, AQU, and CII for the (upper panels) 31 October event, (middle panels) 1 November event, and (bottom panels) aftershock # 7. Theoretical curves are: (solid line) the best fit scaling (19), (dotted line) the 25-bar stress drop scaling, and (dashed line) the stress drop scaling by MM08.

Figure 8 – (Upper panels) Estimate of spectral diminution parameter (κ) for selected stations that recorded the Molise mainshocks. (Lower panel) Comparison between results from Molise records and previous estimates of κ from central and southern Apennines earthquakes (Rovelli *et al.*, 1988). Bars indicate the separation between minimum and maximum slope of the linear fit of the mean acceleration spectrum of each station.

Figure 9 – (a and b) Observed Fourier spectra of ground accelerations of the two mainshocks recorded at stiff sites. (c and d) Estimates of source-radiated acceleration spectra of the mainshocks. The resulting average stress drops are 16 and 12 bars for the 31 October and 1 November shocks, respectively; the ± 1 s.d. uncertainty is represented by the lower shadowed band matching

observations (light gray). The upper shadowed band (darker gray) represents the statistical uncertainty of the stress drop scaling proposed by Malagnini and Mayeda (2008).

Figure 10 - Synoptic view of seismogenic sources and active stress regime in the central-southern Apennines, showing also the focal mechanism of selected instrumental earthquakes (from Fracassi and Valensise, 2007, modified). Seismogenic source data are from DISS Working Group (2007). The stress drop of earthquakes generated by normal faults (e.g. 1980 and 1984 earthquakes) is assessed as ranging between 50 and 80 bars, all sources described as "deep-seated strike-slip" are likely to generate lower stress drop (10 to 20 bars) earthquakes.

Figure A1 – (Left-hand side) Artificial clipping (saturation at ±0.22 cm/s) of the SCV velocity time histories, forced to reproduce the same duration of the saturated portions of seismograms recorded at ARC1. (Right-hand side) Black curves are the spectra of real and saturated waveforms of SCV; the gray curve is the spectrum of the ARC1 record, showing a very similar spectral content. The maximum underestimation due to clipping is in the order of 20% in the lowest part of the investigated frequency band ($f < 5$ Hz).

Figure A2 – Misfit variance resulting from a grid search approach using (a) spectral ratios and (b) Fourier amplitude spectra. The least-mean-square value is found for 8 and 6 bars in (a) and (b), respectively for the fisrt and second mainshock. Note the better resolution of the minimum of the misfit variance when spectral ratios are used.

Rome, 16 July 2009

To: Michel Bouchon, Associate Editor, Bulletin of Seismological Society of America

Dear Editor,

Please find enclosed the manuscript entitled "*Do strike-slip faults of Molise, central-southern Italy, really release a high stress?*", by G. Calderoni, A. Rovelli, G. Milana, and G. Valensise, that we resubmit to your attention after a thorough revision. Please note that we changed some words in the title. In the next pages, we describe how we have changed the text according to the reviewers' requests.

The submitting author certifies that all coauthors know of and concur with submission of this second version of the manuscript.

The authors certify that no results/data/figures in this manuscript have been published/submitted in whole/part elsewhere.

Sincerely yours

Giovanna Calderoni

Istituto Nazionale di Geofisica e Vulcanologia

Via di Vigna Murata, 605

00143 Roma, Italy

E-mail: calderoni@ingv.it

Office phone: (39)(06) 51860451

Fax: (39)(06) 51860507

Response to Reviews
Click here to download Response to Reviews: Response to Reviewers.doc

The main request of both reviewers was a clearer explanation on how stress drop was derived. We therefore changed significantly the description of the method, being much more clear in explaining our best fit procedure. We added an additional Appendix to show also the results of a best fit using Fourier amplitude spectra. Moreover, we shortened the discussion on the use of previous attenuation models published in the literature, and eliminated the discussion on station SNN because recent investigations on local conditions of the station site revealed that it lies on shallow soft materials, although located on a limestone outcrop.

We wish to thank Joe Fletcher and the second anonymous reviewer for their very constructive criticisms.

An explanation follows for each of the reviewers' requests.

Reviewer 1.

General comments

1) Clipped data is a problem. When in the appendix the paper states that the record from SCV is consistent with the record from ARC1, it is not at all clear what is meant by that, amplitudes are the same, spectra look alike? Clearly the records don't overlay except for right around the first S wave arrival, sort of. SMC NS doesn't look anything like ARC1 NS. The spectra are more convincing and maybe the text should focus more on the spectra.

We changed text and figure giving more emphasis to the spectra, and reducing the stress on wave forms in the time domain. A comparison of spectral content at ARC1 and SCV is also shown.

2) In general single station estimates are to be avoided as even ratios may include unknown effects that are not known and not modeled as when the events are not that close to each other. I recognize that other data is used, but with more data, a more comprehensive inversion system could be used (such as Boatwright, BSSA, Oct. 91) that does a better job determining the path effects. With respect to this study I presume that there is no more strong motion data that could be folded into an inversion.

All the available data are used in our manuscript: i) the ARC1 sequence, that is now inverted for the source scaling both in terms of spectral ratios and Fourier amplitude; ii) data of AQU and CII, that are used for a consistency check in terms of spectral ratios; and iii) all the rock-site strong-motion accelerograms, that are used to derive stress drop from the high-frequency source acceleration plateau.

3) If you are going to compare peak acceleration with attenuation models, I would use more than Sabetta and Pugliese. Include either Ambraseys and/or a Boore relation. Boore's is used a lot so it makes for a useful comparison to other investigations. I would suggest the '97 relation and not use the newer NGA stuff, but that is a matter of opinion. I realize there might be differences in regional attenuation, so maybe SEA99 (Spudich et al.) should also be considered.

We have also shown the predictive equations by Boore, Joyner and Fumal (1997) for strike-slip events.

4) Figure 2 shows that inside about 45 km there is quite a lot of scatter to the data. Right around 40 km there is at least an order of magnitude scatter. So it is not quite accurate to state that

the ground motion data is low. I agree that further out the ground motion is low so the author needs to find a reason for the close in scatter some of which is higher than the prediction relation. A single rms number would be low, but that is masking the close versus far change in fit.

Three of the four stations that show the largest values are known to be characterized by large inter-station residuals: LSN, SSV and SNN are affected by strong site effects. Apart from these few cases, the overall scenario is indicative of a low shaking.

5) The data section was not organized well as you will see by the comments below. For example, in the methods section a discussion is given for the processing of accelerometer data that should be in the data section.

We changed the text accordingly.

6) I thought the fits in fig 5 are not that good. The duration in a is not fit well and there are many secondary phases coming in that make it difficult to determine the real S pulse. I guess the authors are trying to make the case that the overall long period fit is good, but that requires a leap of faith. Just because the amplitudes are okay does not justify Figure 5. If the authors only care about the amplitudes then just give the amplitudes.

According to the reviewer's suggestion, that figure has been eliminated (this compensates the addition of one new figure in Appendix B).

7) The spectral ratio method really only works (wave propagation assumptions) if the events are close together. Are they?

We discuss the validity of these assumptions in larger detail in several parts of the text.

8) Pg. 13 When fitting a stress drop, it seems that an assumption about the stress drop of the smaller events is being used. But I guess that the lower events corner is beyond 10 Hz so the method ignores the corner of the smaller events. If this is true please state it somewhere.

We discuss the role of corner frequency of smallest events. In our approach, it must fall inside the frequency band of analysis otherwise the stress drop of smallest event would not be resolved using (4).

9) Pg. 13-14 It is not clear to me why the ratios are interpreted in terms of stress drop and not corner frequency first. I understand that the issue is whether these are large or small stress drop events, but the paper skips an initial step in determining the corner frequency. The problem is that stress drop in a Brune sense cannot be easily interpreted in terms of anything because the Brune model is too simple. So why not just determine corner frequency, which just assumes a ω-squared model and then say if we use a Brune model or Sato model or maybe a Boatwright model what the stress drop is for that corner and moment.

We have explained that the two methods that we use to assess stress drop do not derive it from f_0: the first one derives the scaling law through the coefficients p and q of Eq. 7; the second method assumes that the flat high-frequency plateau of the source acceleration spectrum is proportional to $M_0^{1/3}$ and $\Delta\sigma^{2/3}$ and then depends on $\Delta\sigma$ only, being M_0 known from independent estimates.

10) Pg. 20 The discussion about the other papers seems a bit out of the path of this paper. If the authors want to take on these papers, maybe they should leave that for another day. The statement about crustal velocity not being accurate would need better analysis with actual estimates not just a reference to figure 4.

We deleted that discussion.

Specific comments:

1) Pg. 3 I would not use "sophisticated" to describe the MM08 technique when I believe the authors really mean complicated, convoluted or even hard to follow. Just say "based on coda envelopes."

OK.

2) Pg. 4 20 Hz is a pretty low sample rate and this discussion is not that concise. Please restate so that it is clear what sensors are being used and at what sample rates. The paper should be using the 200Hz sample rate if it is available.

Although telemetered sampling at 100 Hz for stations AQU and CII began on March 2002, the records of Molise earthquakes are only available with the local 20-Hz sampling due to a breakdown of transmission.

3) Pg 5 I found the data section as well as other parts of the paper organized in a way that was hard to follow.

a) The data section lists several data sets in no particular order. But the results mostly use the data from ARC1. So it seems more consistent to discuss the data that will be used the most first.
b) It is clearer at the beginning of the methods section. Is the 10 Hz upper limit to the frequency band high enough to recover the corner frequency of the smaller events? Probably not so the method recovers the lower corner of the larger event. Would a plot showing the original spectra (idealized Brune spectra) for the larger and smaller events, the ratio, and then what band limiting does? Or maybe just a discussion.
c) It seems that at times the jumps back and forth from data to methods regardless of what section we are in. So these two sections need to be rewritten to be better organized and include more detail.

The two sections have been completely rewritten according to the indications. Also the discussion on corner frequencies is included.

4) Pg 7 When computing spectra, were the spectra corrected for differences in window length? The longer the window, the greater the Fourier amplitude.

A comment is added explaining the reason of our choice (to avoid decreasing artificially the stress drop of mainshocks in spectral ratios).

5) Pg. 7 I would use the words "running mean over" instead of "running box".

OK.

6) Pg. 7 The paragraph after eq. 1 is not well organized. After the equation define all of the terms and then discuss the step taken to compute spectra. Spectral dissipation is not a clear description. Just use the word attenuation, which can be from anelastic or scattering; close to the surface or mid-crustal.

We modified the text changing the critical words.

7) Pg. 7 I can surmise what MedNet is but I think it would be better to state that this is the catalog for the local short period net run by …

OK.

8) Pg. 8 The high-pass filter isn't any where near the corner frequencies, right? A table of values might be appropriate here.

We explain that we do not assess stress drop from corner frequency, but from the high-frequency plateau well above the corner frequency. We also mention the values of the high-pass frequencies used in the data processing.

9) Pg. 9 Stress drop is not part of eq. 3. It could be if you combined it with

$$\Delta\sigma = \frac{7}{16}\frac{M_0}{r^3} \qquad \text{and} \qquad r = \frac{2.34\beta}{2\pi f_c}$$

which are very well known, but it should be important to be explicit.

The proper equations are now explicitly written.

10) Pg. 9 It is not clear what is trying to be accomplished with the impedance function. It appears to give an overall amplification function, I guess due to spreading. But why compute the RATTLE response if you only wanted the ray tube spreading function in the first place?

Both functions are now shown in order to visualize their equivalent role.

11) Pg. 10 I am not crazy about describing the Kappa term as a zero distance term. I think it is better to just call it a site term.
12) Pg. 10 If K is 0 then the analysis system to determine this function was not well constrained or over constrained, but maybe the overall function can be used within certain distance ranges. And then the authors discard the Malagnini function anyway. If part of the purpose of this paper is to discredit the MM00 attenuation relation then I suggest being clearer about this (hopefully not a personal attack, but if it doesn't fit the data then it is fair game).
13) Pg. 10 Q is not present in eq. 7 so it is not appropriate to define it (again). If you drop the discussion of the Malagnini relation then define Q after eq. 8.

Comments 11), 12) and 13) were relative to a part of the text that has been deleted in the second version.

14) Pg. 11 The statement that the station is not sensitive to directivity is not well justified.

We rewrote that sentence.

15) Pg. 12 Ω_0 is defined and then not used in eq 10. The equation needs to be written so the variables are explicitly given and then defined.

OK. The equation is explicitly written.

16) Pg, 15 I would not use the word "guarantees".

It is changed to "suggests".

17) Pg. 16 The authors need to keep separate apparent stress and stress drop. They are not the same.

We eliminated the discussion on the apparent stress.

18) Pg. 16 I would not say "common seismological practice". They can just say following Boore the acceleration can be described as … Also this section needs a better intro so the reader knows where this discussion is heading.

OK. The text has been shortened as well.

19) Pg. 18 So I guess the point is to show that MM00 doesn't work. Otherwise why is in the paper?

That part has been deleted.

Reviewer 2.

Comments on the manuscript

1) You mention that the stress drop is proportional to M0 x f0**3, but you never explain where this relation comes from, neither the coefficient. In my opinion, this coefficient is not necessarily the same for each earthquake, so it remains unclear to me how you modify equation (3) and (4) to make the stress drop(s) appear. You should rewrite your equations (3) and (4), as a function of M0 and stress drop, because you are using these explicit formulas to derive the stress drops. What is the coefficient you consider for the absolute spectra of strong motions?

The methods are now explained in details.

2) What is the stress drop given by geodesy (i.e. Giulani et al.) or seismology (Vallée & Di Luccio)? In both cases, you have an estimate of the moment and surface rupture, and so you can use approximate formulas to derive the static stress drop.

The values given by geodetic data are included in the text.

3) The reference to Malagnini & Mayeda is not present in the bibliography!

OK.

4) Figure 5 : It does not seem that the agreement is satisfactory. Maybe it is due to the fact that your source does not include high frequencies

(simple shape with duration ~5s) but in this case you should filter both data and synthetics before comparison. Please comment this point.

The figure has been eliminated being not necessary.

5) Figure 6 is not clear because we do not know which grey fitting curve is in relation with which data curve. Please make this figure clearer.

The missed indication is now provided.

6) You should have labels in all your figures, not only the unities

The missing labels have been added to the figures.

Fig 9

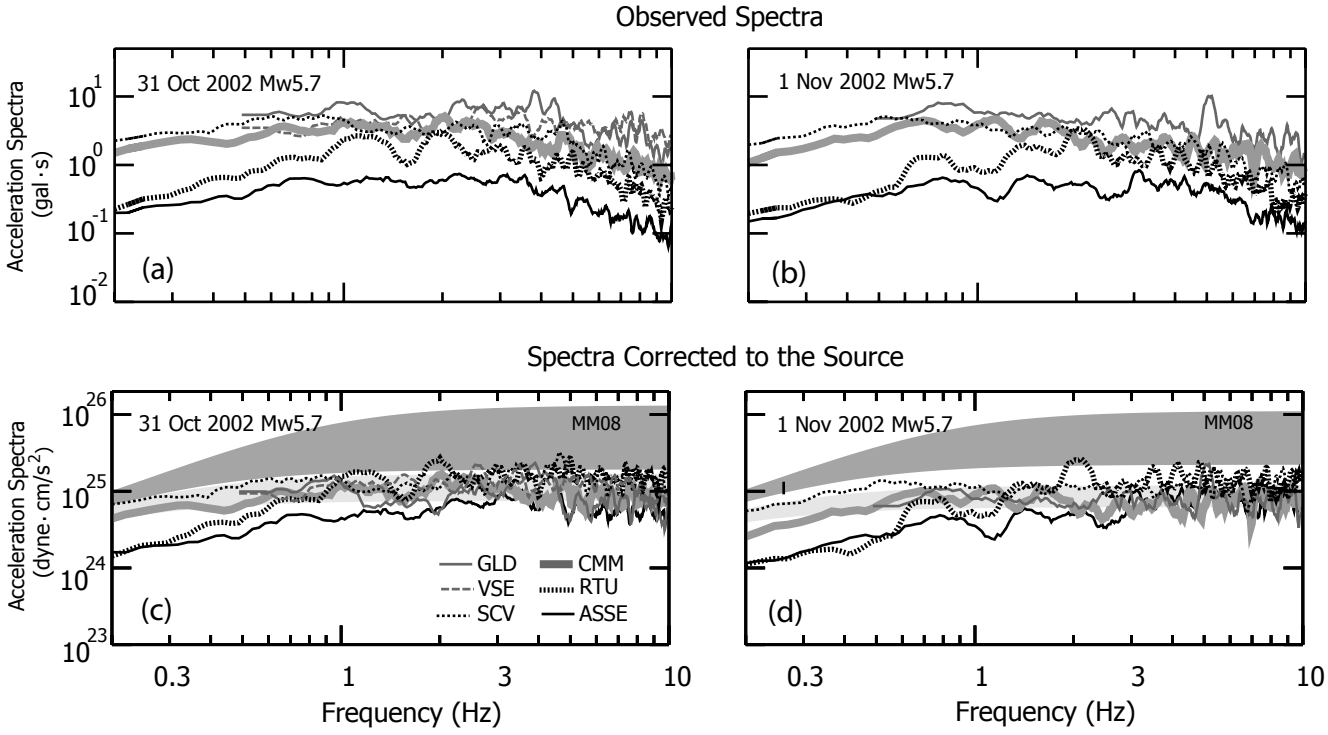
Observed Spectra
31 Oct 2002 Mw5.7
1 Nov 2002 Mw5.7
Acceleration Spectra (gal · s)
(a)
(b)
Spectra Corrected to the Source
31 Oct 2002 Mw5.7
1 Nov 2002 Mw5.7
MM08
Acceleration Spectra (dyne · cm/s²)
GLD
CMM
VSE
RTU
SCV
ASSE
(c)
(d)
0.3
1
3
10
Frequency (Hz)

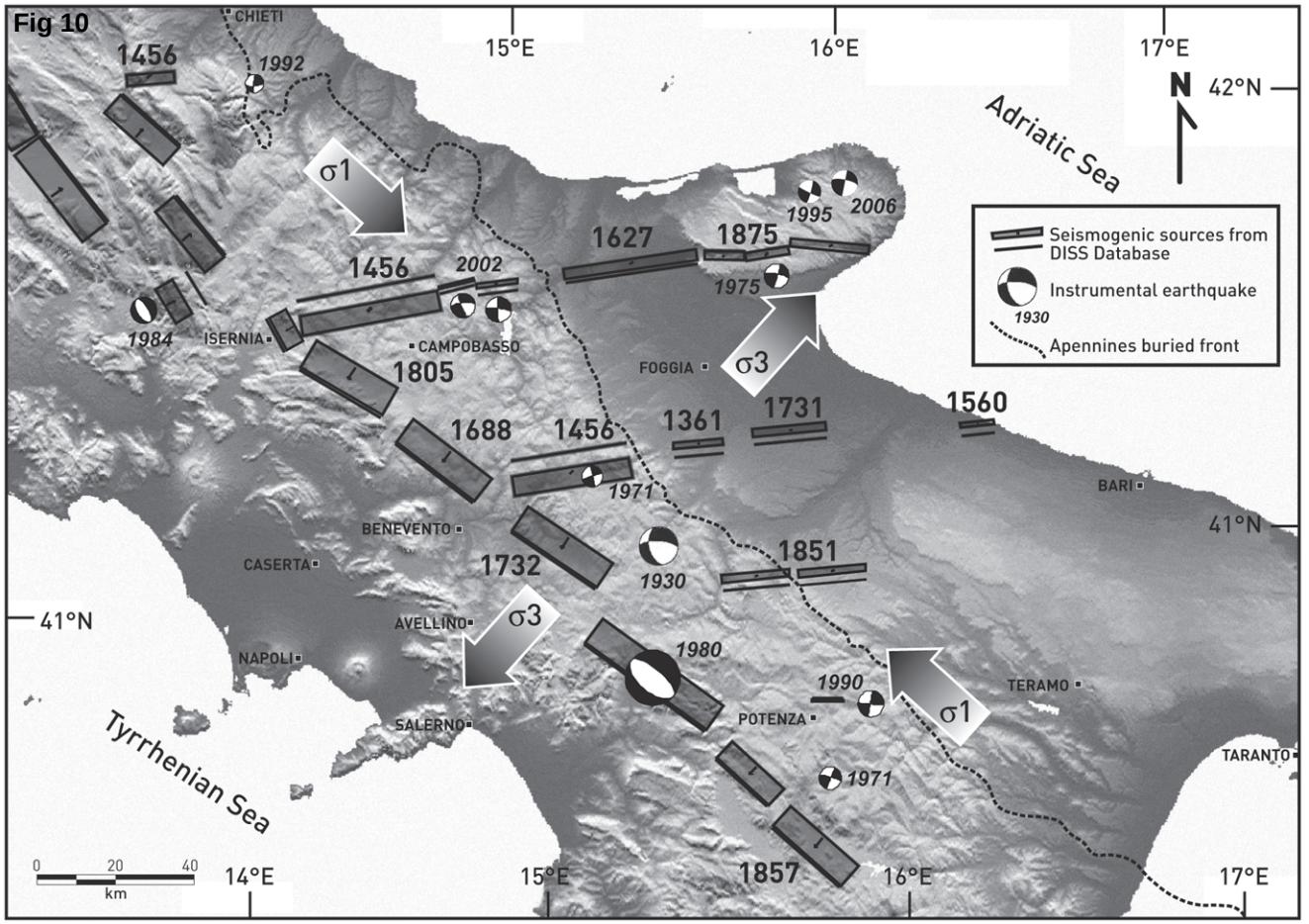
Fig 10
CHIETI
15°E
16°E
17°E
N
42°N
Adriatic Sea
1456
1992
σ1
1995
2006
1627
1875
1456
2002
1975
1984
ISERNIA
CAMPOBASSO
1805
FOGGIA
σ3
1731
1560
1688
1456
1361
1971
BARI
BENEVENTO
41°N
CASERTA
1732
1930
1851
41°N
AVELLINO
σ3
1980
NAPOLI
1990
TERAMO
POTENZA
σ1
SALERNO
Tyrrhenian Sea
TARANTO
1971
0
20
40
km
14°E
15°E
1857
16°E
17°E
Seismogenic sources from DISS Database
Instrumental earthquake
1930
Apennines buried front

Fig A1

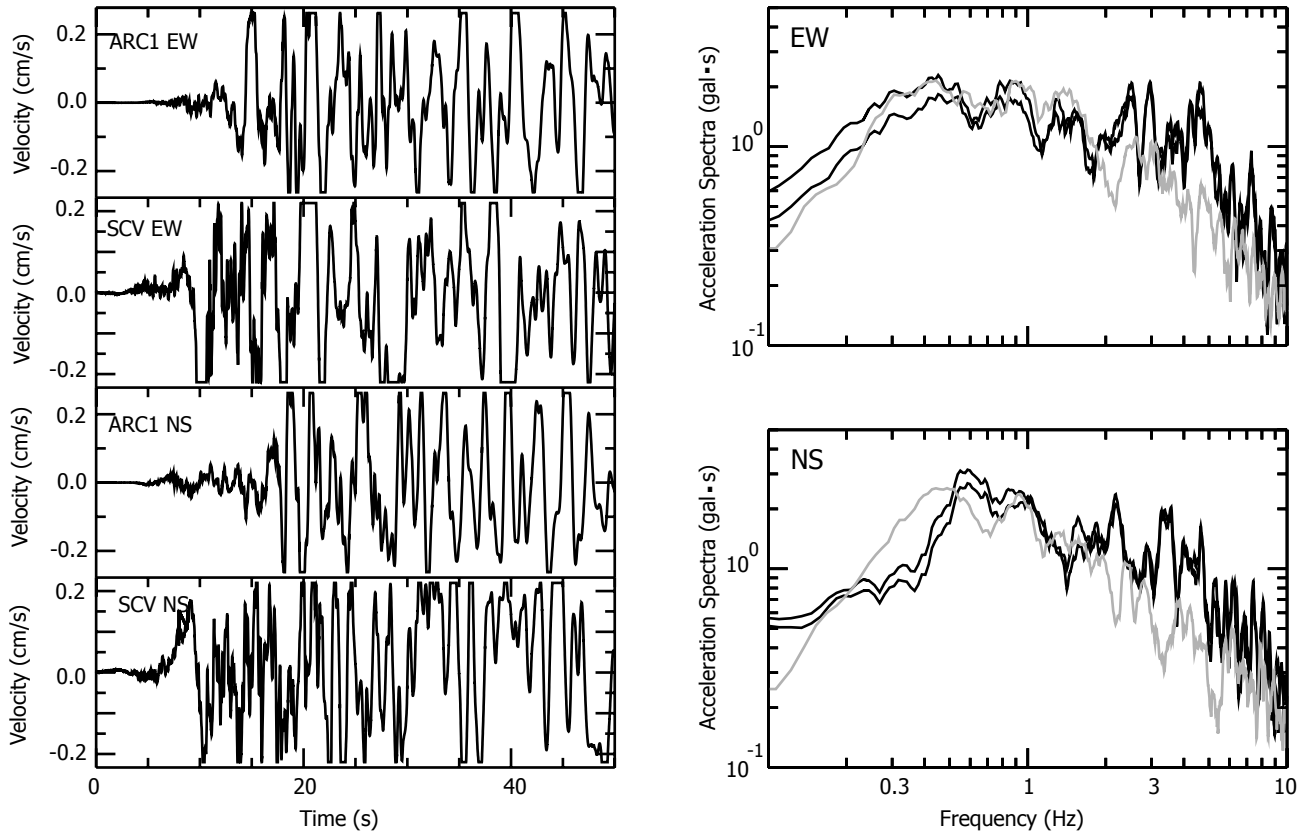
ARC1 EW
SCV EW
ARC1 NS
SCV NS
Velocity (cm/s)
0.2
0.0
-0.2
0
20
40
Time (s)
EW
NS
Acceleration Spectra (gal•s)
10^0
10^{-1}
0.3
1
3
10
Frequency (Hz)

Fig A2

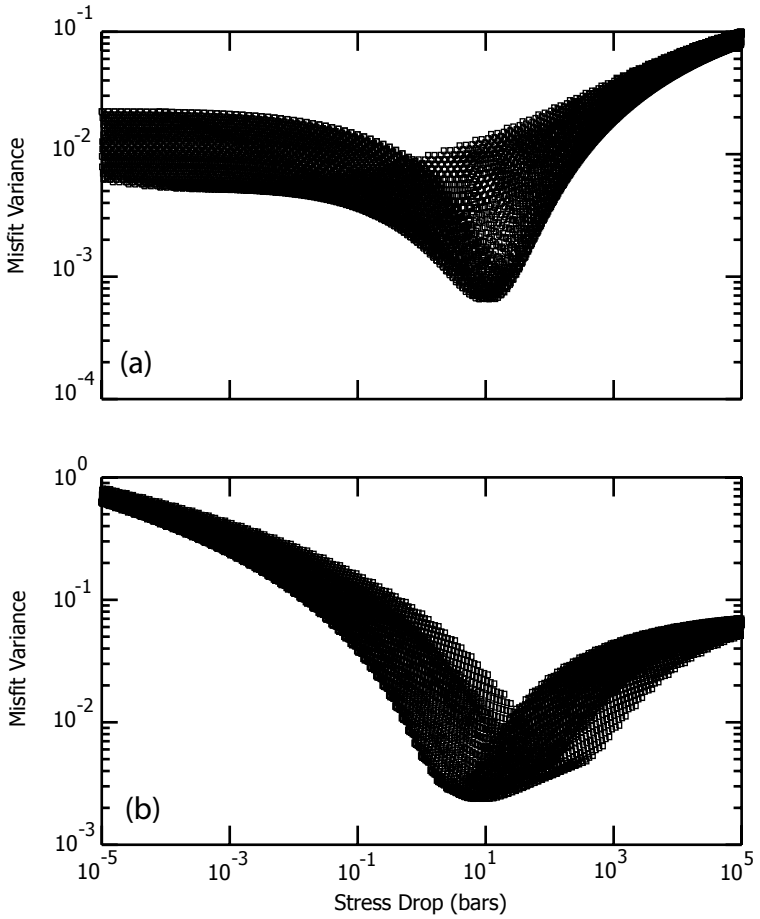

Fig 1

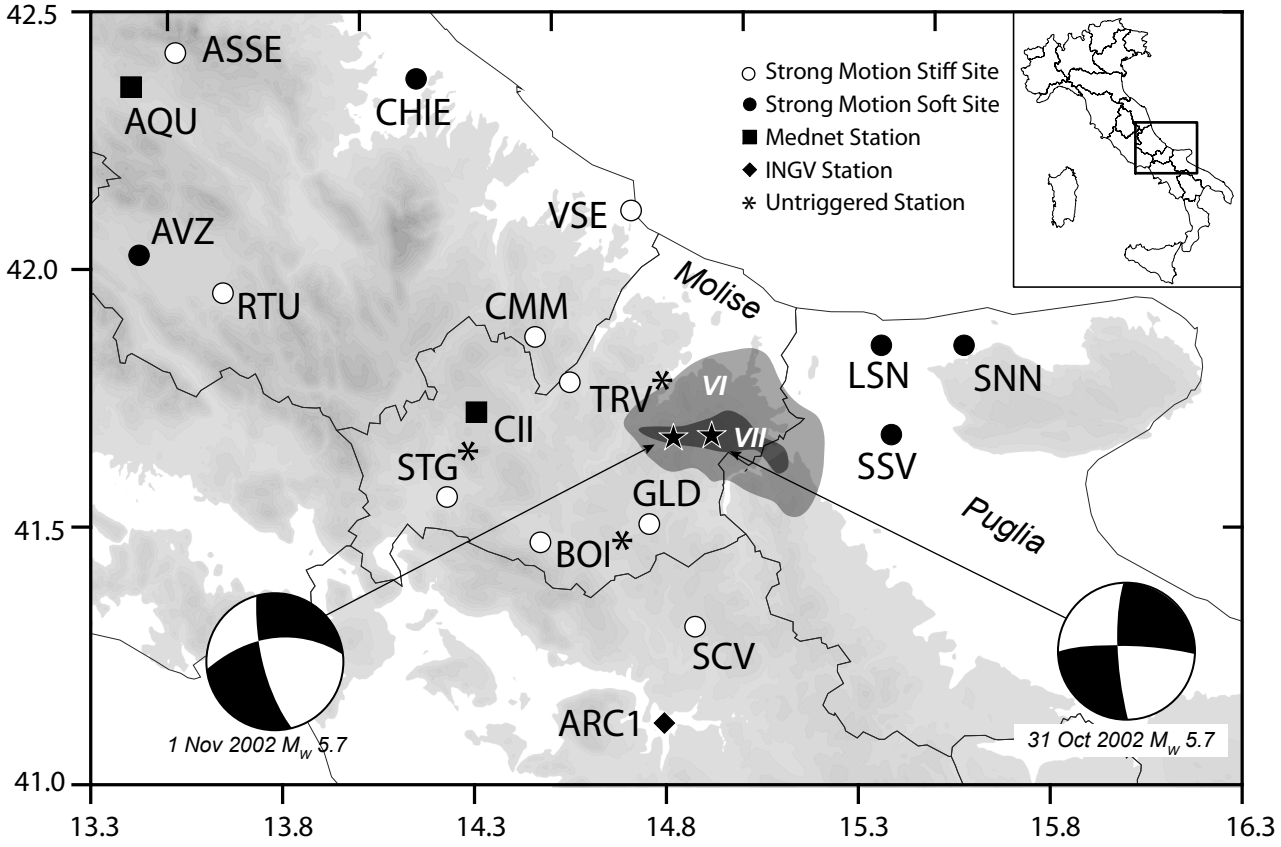
Strong Motion Stiff Site
Strong Motion Soft Site
Mednet Station
INGV Station
Untriggered Station
ASSE
AQU
CHIE
AVZ
VSE
RTU
CMM
Molise
TRV
VI
VII
CII
STG
LSN
SNN
SSV
GLD
Puglia
BOI
SCV
ARC1
1 Nov 2002 M_w 5.7
31 Oct 2002 M_w 5.7
42.5
42.0
41.5
41.0
13.3
13.8
14.3
14.8
15.3
15.8
16.3

Fig 2

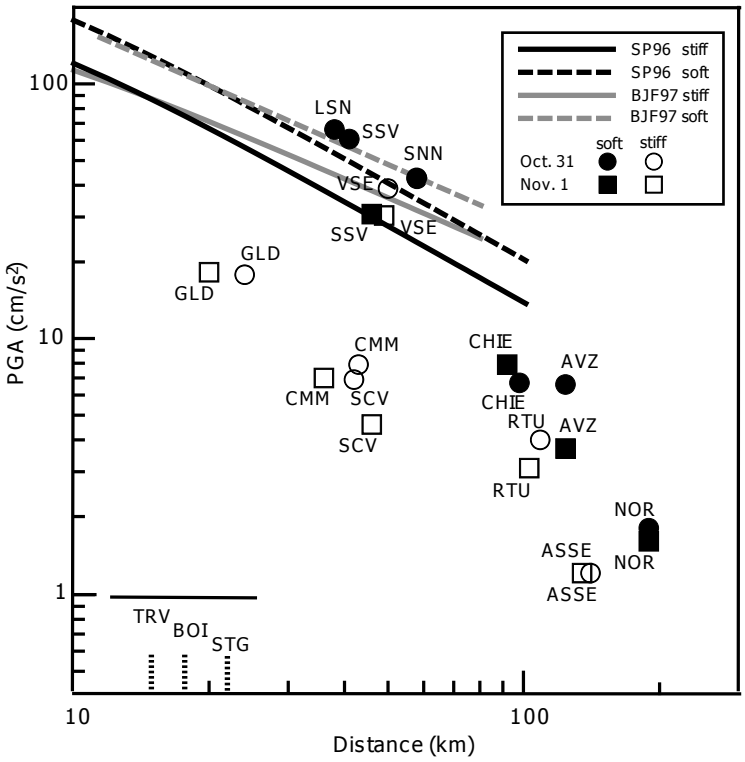
SP96 stiff
SP96 soft
BJF97 stiff
BJF97 soft
soft stiff
Oct. 31
Nov. 1
100
10
1
PGA (cm/s²)
LSN
SSV
SNN
VSE
SSV
VSE
GLD
GLD
CMM
CMM
SCV
SCV
CHIE
CHIE
AVZ
RTU
AVZ
RTU
NOR
NOR
ASSE
ASSE
TRV
BOI
STG
10
100
Distance (km)

Fig 3

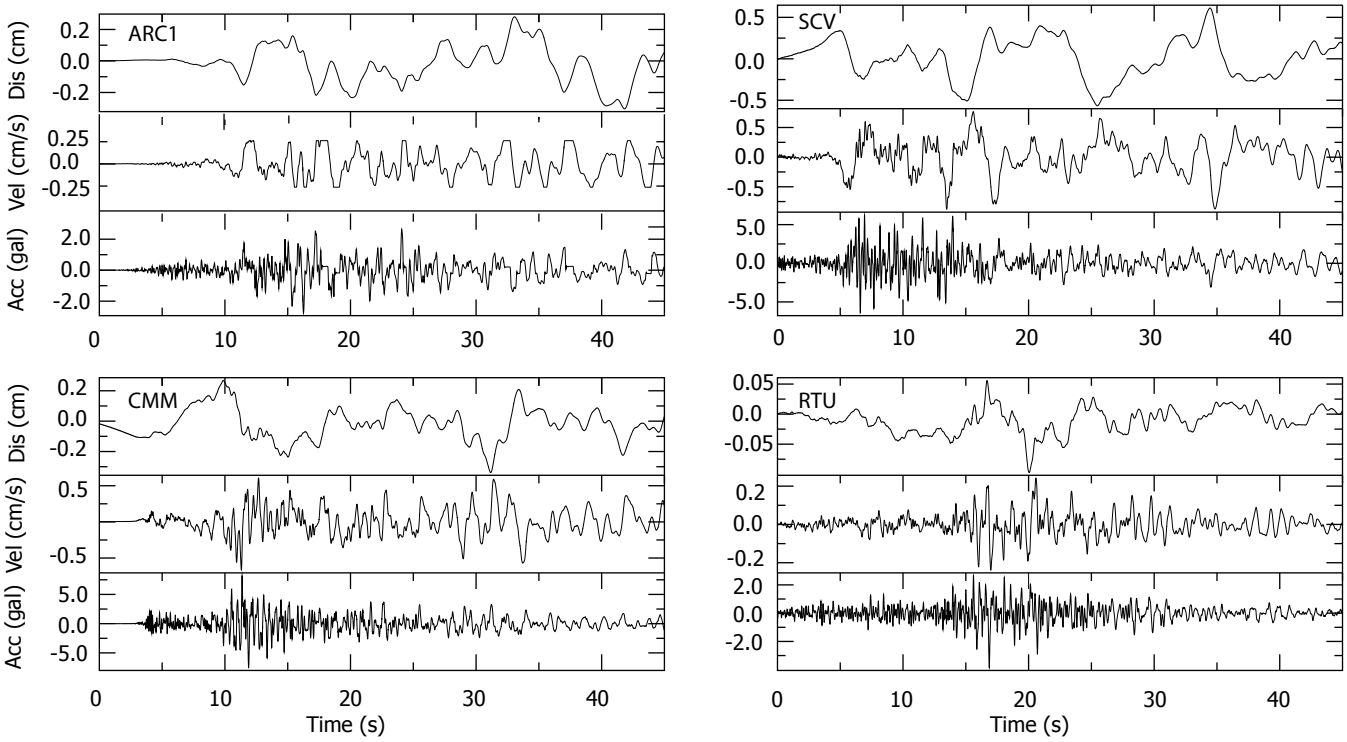

Fig 4

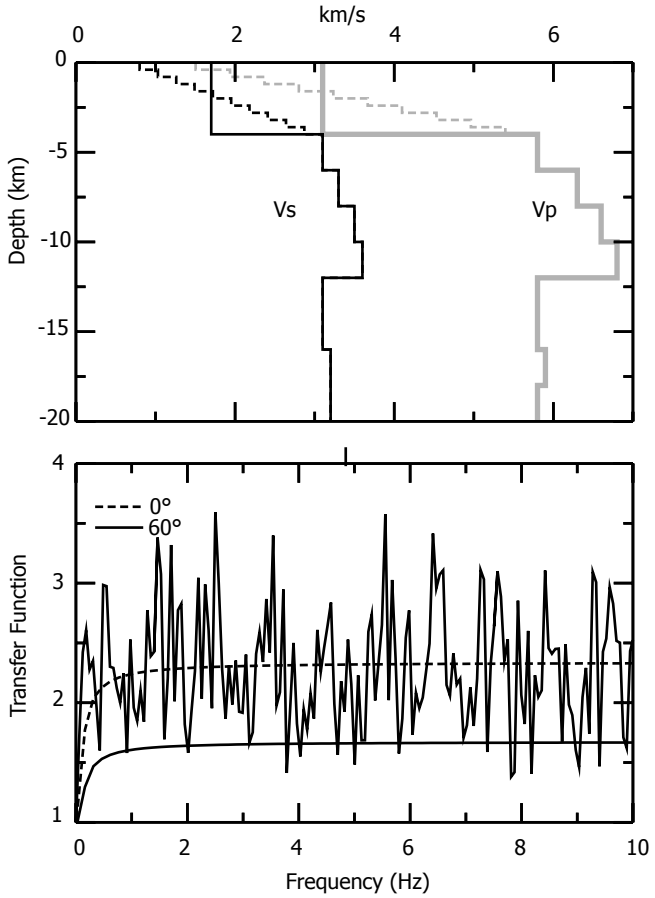
km/s
0
2
4
6
0
-5
-10
-15
-20
Depth (km)
Vs
Vp
4
3
2
1
Transfer Function
0°
60°
0
2
4
6
8
10
Frequency (Hz)

Fig 5

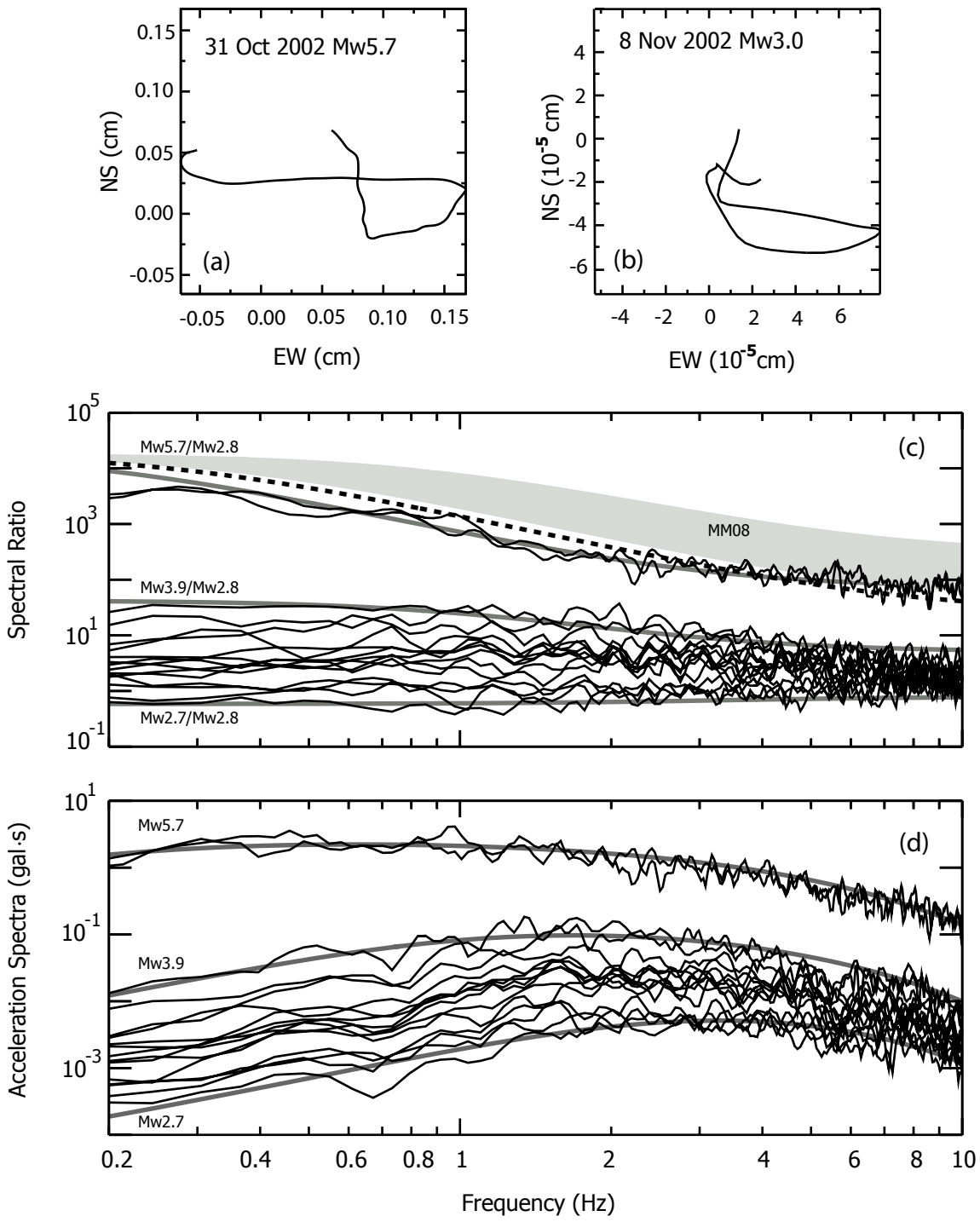
31 Oct 2002 Mw5.7
NS (cm)
EW (cm)
(a)
8 Nov 2002 Mw3.0
NS (10-5 cm)
EW (10-5cm)
(b)
Spectral Ratio
Mw5.7/Mw2.8
MM08
Mw3.9/Mw2.8
Mw2.7/Mw2.8
(c)
Acceleration Spectra (gal·s)
Mw5.7
Mw3.9
Mw2.7
(d)
Frequency (Hz)

Fig 6

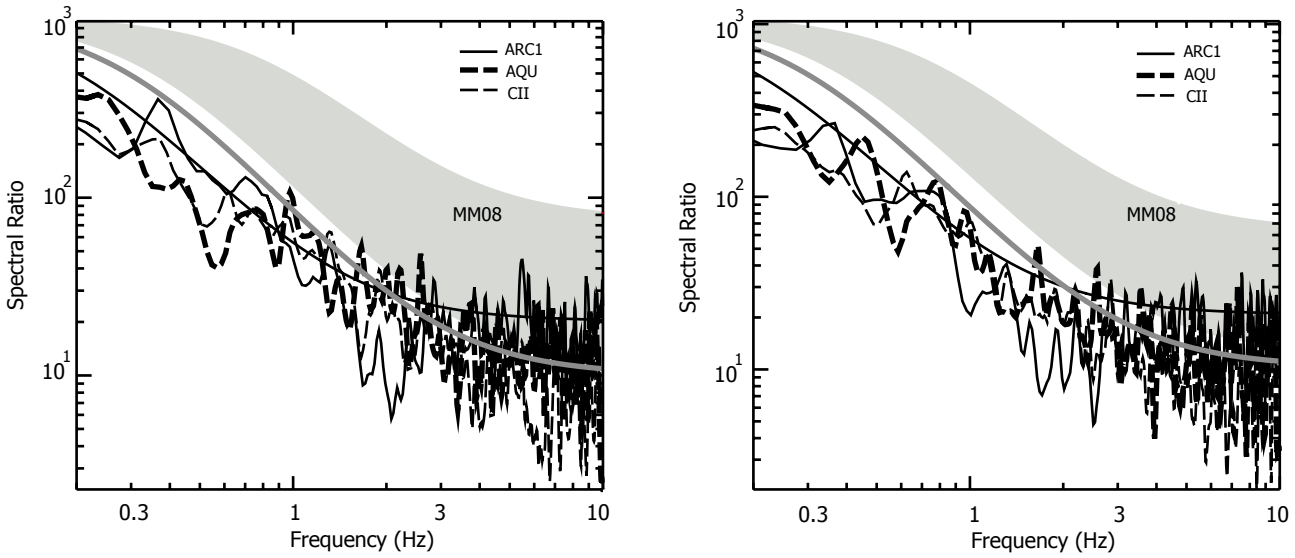

Fig 7

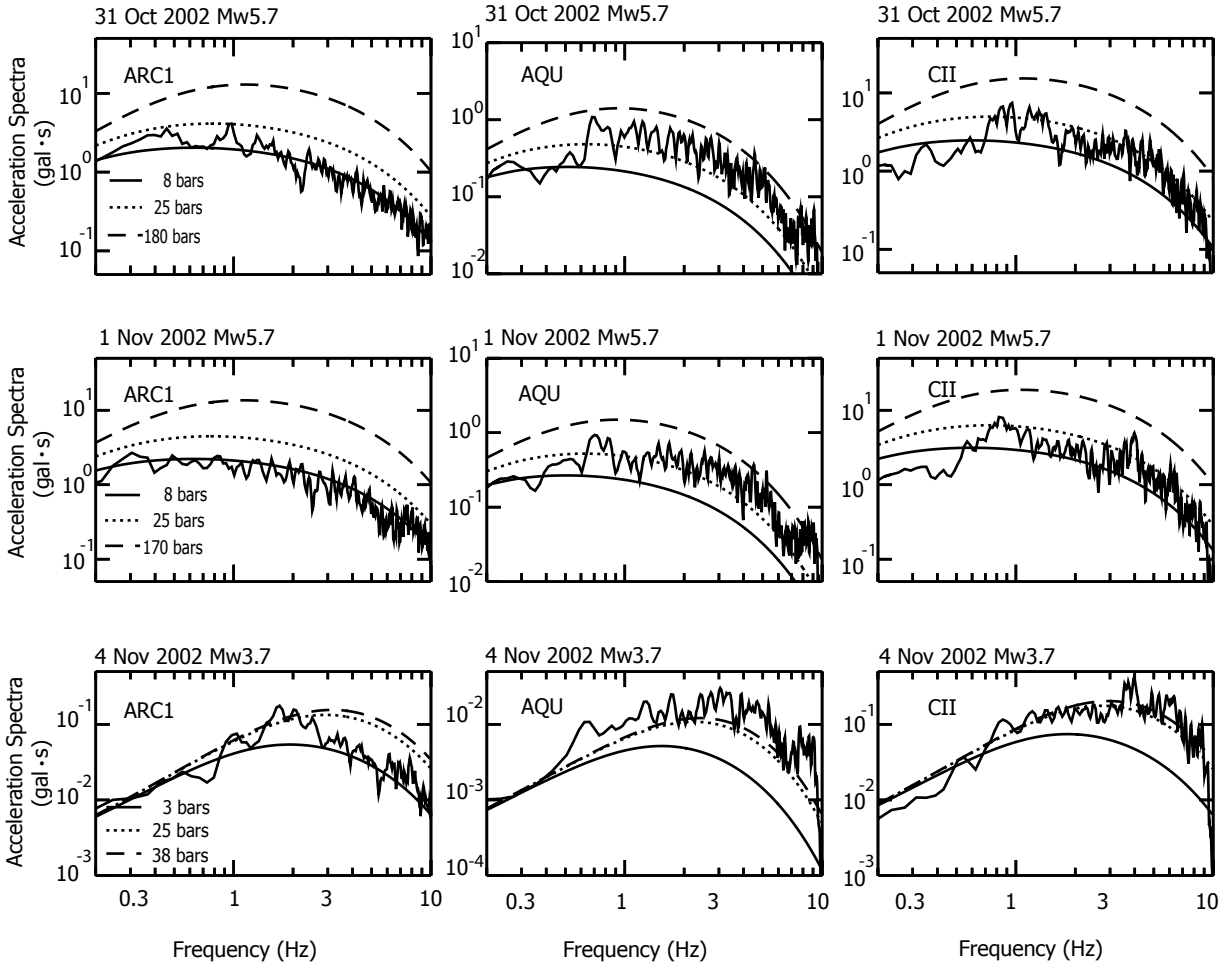
31 Oct 2002 Mw5.7
ARC1
AQU
CII
1 Nov 2002 Mw5.7
4 Nov 2002 Mw3.7
Acceleration Spectra (gal・s)
8 bars
25 bars
180 bars
170 bars
3 bars
38 bars
0.3
1
3
10
Frequency (Hz)

Fig 8

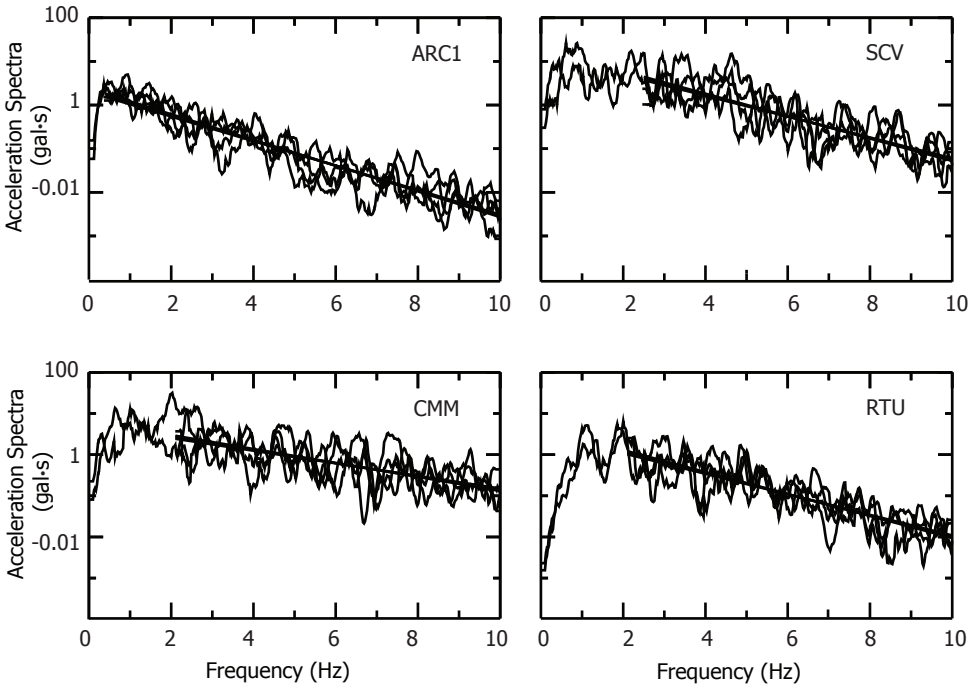
ARC1
SCV
CMM
RTU
Acceleration Spectra (gal·s)
100
1
-0.01
0
2
4
6
8
10
Frequency (Hz)

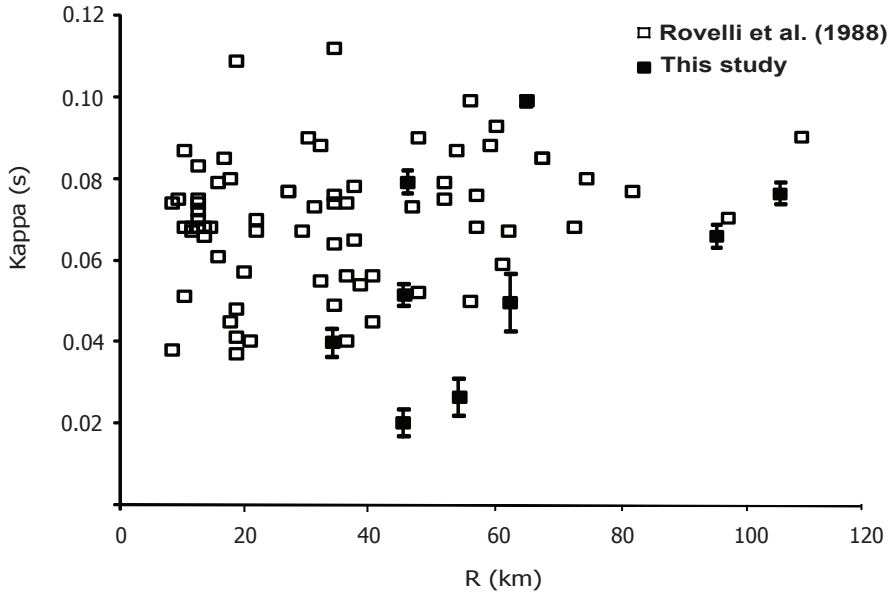
Rovelli et al. (1988)
This study
Kappa (s)
0.12
0.10
0.08
0.06
0.04
0.02
0
20
40
60
80
100
120
R (km)

Table

TABLE 1. List of earthquakes considered in this study

Event	*Date 2002*	*Time,UTC*	*Lat N*	*Long E*	M_0 *(dyne·cm)*	M_w
1	31 Oct	1032	41.682	14.897	$4.3 \cdot 10^{24}$	5.7
2	1 Nov	0945	41.734	14.805	$2.8 \cdot 10^{20}$	2.9
3	1 Nov	1509	41.719	14.840	$4.6 \cdot 10^{24}$	5.7
4	1 Nov	1611	41.716	14.830	$2.0 \cdot 10^{20}$	2.8
5	1 Nov	1850	41.639	14.844	$1.4 \cdot 10^{20}$	2.7
6	2 Nov	0621	41.700	14.804	$1.6 \cdot 10^{21}$	3.4
7	4 Nov	0326	41.741	14.805	$4.2 \cdot 10^{21}$	3.7
8	4 Nov	0928	41.724	14.864	$7.5 \cdot 10^{20}$	3.2
9	5 Nov	2310	41.714	14.934	$3.1 \cdot 10^{21}$	3.6
10	8 Nov	0353	41.620	14.927	$3.5 \cdot 10^{20}$	3.0
11	9 Nov	1340	41.682	14.833	$6.4 \cdot 10^{20}$	3.1
12	10 Nov	1223	41.665	14.834	$5.5 \cdot 10^{20}$	3.1
13	11 Nov	1832	41.664	14.873	$1.0 \cdot 102^{1}$	3.3
14	12 Nov	1346	41.659	14.790	$7.3 \cdot 10^{20}$	3.2
15	13 Nov	0252	41.715	14.817	$7.7 \cdot 10^{20}$	3.2
16	2 Dec	2053	41.668	14.855	$1.0 \cdot 10^{22}$	3.9